CONTRIBUTIONS FROM THE MUSEUM OF PALEONTOLOGY

THE UNIVERSITY OF MICHIGAN

VOL. 29, NO. 9, PP. 201-257 November 30, 1995

MORPHOLOGICAL, CRYSTALLOGRAPHIC, AND STRATIGRAPHIC DATA IN CLADISTIC ANALYSES OF BLASTOID PHYLOGENY

BY

BRIAN E. BODENBENDER

MUSEUM OF PALEONTOLOGY
THE UNIVERSITY OF MICHIGAN
ANN ARBOR

CONTRIBUTIONS FROM THE MUSEUM OF PALEONTOLOGY

Philip D. Gingerich, Director

This series of contributions from the Museum of Paleontology is a medium for publication of papers based chiefly on collections in the Museum. When the number of pages issued is sufficient to make a volume, a title page and a table of contents will be sent to libraries on the mailing list, and to individuals on request. A list of the separate issues may also be obtained by request. Correspondence should be directed to the Museum of Paleontology, The University of Michigan, Ann Arbor, Michigan 48109-1079.

VOLS. 2-29. Parts of volumes may be obtained if available. Price lists are available upon inquiry.

MORPHOLOGICAL, CRYSTALLOGRAPHIC, AND STRATIGRAPHIC DATA IN CLADISTIC ANALYSES OF BLASTOID PHYLOGENY

By

BRIAN E. BODENBENDER

Abstract—The echinoderm class Blastoidea is well-suited for evolutionary studies, but the phylogeny of the group is incompletely known. This paper presents morphological data for 68 blastoid genera, each represented by a single species, as a basis for parsimony-based phylogenetic analysis.

Interpretation of complex morphological features and their distillation into entries in a character-by-taxon data matrix are critical to the outcome of subsequent phylogenetic analyses. While the preferred coding of blastoid characters was identified prior to data analysis, additional cladistic analyses of both a limited subset of taxa and the full data set explore the sensitivity of the results to alternative character coding decisions. Congruence with an independent data set, the order of occurrence of blastoid fossils in the stratigraphic record, is useful for evaluating the results of competing analyses, but in this case does not point to one set of coding decisions as decidedly superior to alternatives. In general, the results show that coding decisions that alter the relative weighting of characters or hypothesize a more structured series of evolutionary transitions between character states yield more structured results.

Stratigraphic data are more decisive in sorting among equally-parsimonious cladograms issuing from a single analysis. Of the 14,498 cladograms resulting from the preferred coding of blastoid morphology, 96 were found to be most congruent with the blastoid stratigraphic record.

Orientations of crystallographic axes in blastoid skeletal elements are as phylogenetically informative as other morphological characters, and can therefore serve as useful data in phylogenetic studies of echinoderms.

The morphological data presented here and explored with cladistic analysis can also be employed in stratocladistic analysis. When all data are taken into account, stratocladistic analysis, which considers both morphological and stratigraphic data, can be expected to provide a more parsimonious hypothesis of blastoid phylogeny than does cladistic analysis, which considers morphology alone.

INTRODUCTION

Blastoids, a class of sessile, stemmed Paleozoic echinoderms, have been the subject of numerous phylogenetic (Breimer and Macurda, 1972; Waters et al., 1985; Horowitz et al., 1986; Waters and Horowitz, 1993), paleoecological (Waters, 1990), and morphological studies (Olson and Miller, 1958; Foote, 1991) for the past several decades. Still, despite detailed

phylogenetic work on various subsets of blastoids and their continuing usefulness in a variety of evolutionary studies, the overall phylogenetic relationships within the class have yet to be discovered. This paper develops an overview of phylogenetic relationships among blastoid genera using parsimony-based cladistic analysis.

Character recognition is crucial to phylogenetic analysis, so one goal of this contribution is to present in detail an interpretation of blastoid morphology for use in cladistic and other analyses of phylogeny. Matters of character coding and weighting are as critical to the outcome of cladistic studies as is the initial recognition of characters, so this paper explores the results of several alternative treatments of morphological data before analyzing characters under the preferred coding and weighting protocol. In comparing the results of alternative analyses, congruence with the order of occurrence of fossils in the stratigraphic record is used as an independent criterion for assessing the relative performance of different data treatments. Stratigraphic data are also useful for choosing among hypotheses that are equally supported according to morphological data alone (Suter, 1993, 1994). This sorting of equally-parsimonious hypotheses by stratigraphic congruence is used to select a set of best-supported phylogenies resulting from cladistic analysis of morphological characters. In conjunction with the investigation of alternative interpretations of blastoid morphology, this paper also assesses the impact of a new data set, the orientations of crystallographic axes in blastoid skeletal elements, on the phylogenetic analysis.

This paper does not, however, evaluate either character evolution or blastoid systematics using the cladistic results. The primary interest in developing the cladistic hypotheses is to provide a starting point for stratocladistic analyses (Fisher, 1982, 1991, 1992, 1994a,b). Stratocladistic methods, which go beyond "sorting by stratigraphic congruence", can be expected to provide more parsimonious interpretations of blastoid evolutionary history when both morphological and stratigraphic data are considered than do cladistic analyses of morphological data alone.

The Treatise on Invertebrate Paleontology (Beaver, Fay, Macurda, Moore, and Wanner, 1967) explained the detailed anatomy of blastoids and presented standard conventions for orienting specimens and labelling the pentamerally-symmetrical parts of the blastoid theca. Breimer and Macurda (1972) subsequently reinterpreted some aspects of anatomy and revised some anatomical terms. Where conflicts in usage exist, this paper uses the revised terminology. Several features identified by common morphological terms, however, are reinterpreted herein or are described as characters indirectly through their relationships to other structural features. In developing a cladistic hypothesis of generic relationships within the blastoids, this contribution presents data on 94 morphological characters for blastoids. Many of these are characters that previous workers considered important, as suggested by their inclusion in generic, familial, and ordinal diagnoses. In addition, morphological features less frequently cited as taxonomically useful have also been given the opportunity to contribute phylogenetic information. Among these are the orientations of the crystallographic axes in the calcite of blastoid skeletal elements. Work on echinoids (Raup, 1962a,b) and edrioasteroids (Bodenbender, 1990) has demonstrated the potential of crystallographic data to contribute to phylogenetic analyses, and the crystallography of stylophorans has been applied to questions of homology in order to test particular phylogenetic hypotheses (Fisher and Cox, 1987, 1988). This paper examines crystallographic axis orientations as characters within the larger context of the cladistic analysis of blastoid phylogeny.

CLADISTIC ANALYSIS

Previous analyses of blastoid phylogeny used detailed study of morphological characters and a strict ordering of taxa by stratigraphic occurrence to develop hypotheses of character transition and identify primitive and advanced conditions or grades shared by distantly related

species across several lineages. The analysis presented here also relies on detailed morphological study, but compares the resulting observations using parsimony-based cladistic methods. Hypotheses of relationship that are based on a few important characters, as previous hypotheses of blastoid relationships have been, structure the distribution of other characters not included in the initial analysis. In cladistic analyses the implications of a particular phylogenetic hypothesis for the evolutionary history of all characters are made explicit, and these implications can be evaluated and weighed against scenarios of character evolution implied by alternative phylogenetic hypotheses. Cladistic analysis also provides the opportunity for new characters to play a role in elucidating relationships without entirely dismissing the evidence of characters that are important in current classifications and phylogenetic schemes. This aspect of cladistics allows competing evidence to be weighed in determining the best-supported hypothesis of relationships. Cladistic analyses can provide a broad overview of relationships in a group of taxa without relying on hypotheses of character transformation in key characters to structure the analysis. The general statement of relationships may then be tested or expanded by further, detailed work.

The exercise of conducting a cladistic analysis also has some advantages over approaches that seek to elucidate trends in character evolution first and then apply them to phylogenetic hypotheses. A character matrix summarizes previous observations and invites more thorough examination of characters by seeking to use each observation made on individual specimens as the basis for similar observations on all other specimens. This may prompt comparisons that were not initially obvious. Such comparisons can lead to reinterpretation of characters by encouraging the observer to seek relationships between morphologically diverse specimens.

While cladistic analyses are useful and informative of themselves, the data gathered for cladistic studies can also be incorporated into stratocladistic analyses. Stratocladistics combines morphological and stratigraphic data to develop and compare phylogenetic hypotheses. A stratocladistic hypothesis of blastoid relationships is developed and examined elsewhere (Bodenbender and Fisher, ms.).

SPECIMENS

This analysis examines one species from each of 67 blastoid genera (Table 1), representing nearly two thirds of blastoid generic diversity. Subsequent to analysis of these taxa, data were gathered for an additional species, *Macurdablastus uniplicatus*, the oldest known blastoid. Data from all species are coded as characters (Table 2), but *Macurdablastus*, for which many characters could not be coded, was not included in the analyses reported here.

Several different echinoderm groups, including eocrinoids (Sprinkle, 1973) and edrioblastoids (Fay, 1967), have previously been hypothesized to have given rise to the blastoids. Recent opinion, however, has reached a consensus that the coronate crinoids (the Class Coronoidea of Brett et al., 1983) are the group most closely related to blastoids (Sprinkle, 1980; Brett et al., 1983; Paul and Smith, 1984) or are the sister group to [blastoids + *Lysocystites*] (Donovan and Paul, 1985). A close relationship between blastoids and coronates has also been suggested by a preliminary, parsimony-based analysis of the phylogenetic relationships of early echinoderm groups (Bodenbender, unpublished data). Four species of the coronate genus *Stephanocrinus* Conrad, 1842 are used as outgroups for this study. Three of these, *S. gemmiformis*, *S. hammeli*, and *S. osgoodensis*, while morphologically very similar to one another, are distinct from the genotype, *S. angulatus*, and perhaps would be more properly referred to *Cupulocorona* Donovan and Paul, 1985.

Because of limited material, this study does not explicitly address issues of variability within populations, species, or genera. When variation among specimens was noted it was taken into account during the definition and coding of characters, but no systematic survey of variation was attempted for each character. Likewise, specimens were not systematically assessed for

TABLE 1—Blastoid species examined in the cladistic analyses. Representative specimens or those helpful in some aspect of character coding are indicated by museum specimen numbers. Many other specimens were examined in addition to those listed. The main monographic sources of character information for this study were Breimer and Macurda (1972), Macurda (1983), the Treatise on Invertebrate Paleontology (Beaver, Fay, Macurda, Moore, and Wanner, 1967), and Fay (1961b), although the broad focus and schematic format of the latter two sources limit the amount of detailed information they provide on species attributes. Literature citations following a species refer to publications other than the above that were pertinent to the coding of the taxon. Institutional abbreviations are as follows: BB/AF, specimens in the private collection of Alex Fabian of Temperance, Michigan; MCZ, Museum of Comparative Zoology, Harvard University, Cambridge; UM, University of Michigan Museum of Paleontology, Ann Arbor; USNM, United States National Museum, Washington, D.C.

Species	Instructive specimens	References
Stephanocrinus angulatus	UM 66677	Brett et al., 1983; Donovan and Paul, 1985
Stephanocrinus gemmiformis	MCZ 101696	
Stephanocrinus hamneli	UM S5660, 66678	
Stephanocrinus osgoodensis	USNM 42363	
Ambolostoma baileyi	BB/AF 3	Peck, 1930
Angioblastus wanneri	UM 54890, 60670, 60671, 66680	
Anthoblastus stelliformis	UM 58234	
Arcuoblastus shumardi	MCZ 375	Macurda, 1977b; Ausich and Meyer, 1988
Astrocrinus tetragonus	MCZ 362; USNM S3786	Macurda, 1977a
Auloblastus clinei	BB/AF 4; USNM 160567	Beaver, 1961b
Austroblastus whitehousei	UM 62361, 62362	
Brachyschisma corrugatum	UM 57549; BB/AF 5	
Calycoblastus tricavatus	UM 58190	Breimer and Macurda, 1965; Macurda, 1972; Breimer, 1988a
Caryoblastus bohemicus	UM 66632	Breimer et al., 1968
Codaster acutus	UM 57132, 66633	
Cordyloblastus eifelensis	MCZ 195, 305, 213, 101693-101695	Breimer and Dop, 1975
Costatoblastus sappingtonensis	MCZ 554a	Sprinkle and Gutschick, 1967
Cribroblastus cornutus	BB/AF 6; UM 62141	Macurda, 1978; Ausich and Meyer, 1988
Cryptoblastus melo	UM 5452, 5459, 66634	Macurda, 1962
Cryptoschisma schultzii	UM S5740, 56511, 66635	
Decaschisma pulchellum	UM 61803, USNM S3212	
Decemoblastus melonoides	BB/AF 7, 8	Macurda, 1977b; Ausich and Meyer, 1988
Deliablastus cumberlandensis	BB/AF 9-11	Ausich and Meyer, 1988
Deltoblastus permicus	UM 51205, 66636-66646	Breimer and Van Egmond, 1968
Dentiblastus sirius	MCZ 379	Macurda, 1964a
Devonoblastus whiteavesi	UM 56507, 51720, 60589	
Diploblastus glaber	MCZ 1080	Breimer, 1988b
Elaeacrinus venustus	MCZ 101689	
Eleutherocrinus cassedayi	UM 44154, 60592, MCZ 101682	Millendorf, 1979
Ellipticoblastus ellipticus	UM 66647-66650	Etheridge and Carpenter, 1886; Breimer and Joysey, 1968

Euryoblastus veryi	USNM S3784	Ausich and Meyer, 1988
Globoblastus norwoodi	UM S-5747, MCZ 101684	Beaver, 1961a
Granatocrinus granulatus	USNM S3750	Ausich and Meyer, 1988
Hadroblastus whitei	MCZ 1004, UM 59712, 59713, 62308	
Heteroblastus cumberlandi	BB/AF 12-14	Etheridge and Carpenter, 1886
Heteroschisma subtruncatum	UM 66651, 66652	
Hyperoblastus filosus	UM 35035, 66653-66662	Breimer and Dop, 1975
Katoblastus konincki	MCZ 1075	Macurda, 1967
Koryschisma elegans	MCZ 915-961	Sprinkle and Gutschick, 1990
Leptoschisma lorae	USNM 16708, 160712	
Lophoblastus inopinatus	MCZ 1077	Macurda, 1962
Macurdablastus uniplicatus	USNM 359645-359651	Broadhead, 1984
Mesoblastus crenulatus	MCZ 328, 536b	Macurda, 1967
Metablastus wortheni	MCZ 101690-101692	
Monadoblastus granulosus	UM 58184, 66663	Ausich and Meyer, 1988
Monoschizoblastus rofei	UM 57130, 66664	Cline, 1936; Fay, 1961a
Montanablastus baldyensis	MCZ 886-894, 995-997	Sprinkle and Gutschick, 1990
Nannoblastus pyramidatus	UM 62016, 66665	
Notoblastus stellaris	UM 58683	
Nucleocrinus meloniformis	UM 30742, 37483, 66666	
Orbiblastus hoskynae	UM 56556	Macurda, 1965
Orbitremites derbiensis	UM 51812, 57132, 66667-66670	Breimer and Joysey, 1968
Orophocrinus stelliformis	UM 66671	Macurda, 1966
Pentremites godoni	UM 62019, 66672	Macurda, 1975
Pentremitidea archiaci	UM 56514, 66673	
Pentremoblastus conicus	BB/AF 1	Fay and Koenig, 1963
Perittoblastus liratus	BB/AF 15	Ausich and Meyer, 1988
Phaenoblastus caryophyllatus	MCZ 101683	Macurda, 1967
Phaenoschisma laeviculum	MCZ 1001, 101688, 101689, UM 66679	Macurda, 1964b
Placoblastus ehlersi	UM 26427	
Pleuroschisma lycorias	UM 56499, USNM 160716	
Polydeltoideus enodatus	UM 37806, 43930	
Poroblastus granulosus	UM 66674, 47979	
Pterotoblastus gracilis	UM 57451	
Ptychoblastus pustulosus	BB/AF 16, 17	Fay, 1960
Schizoblastus sayi	MCZ 101685, 101686	Cline, 1936; Macurda, 1979
Schizotremites kopfi	BB/AF 18-20	Fay, 1961c; Breimer, 1988a
Strongyloblastus petalus	BB/AF 2, 21, 22	Fay, 1962; Macurda and Breimer, 1977
Tanaoblastus roemeri	UM 66675	
Timoroblastus coronatus	UM 51558	
Tricoelocrinus woodmani	BB/AF 23-26	
Troosticrinus reinwardti	UM 51599, 51602, 66676	Breimer, 1988a

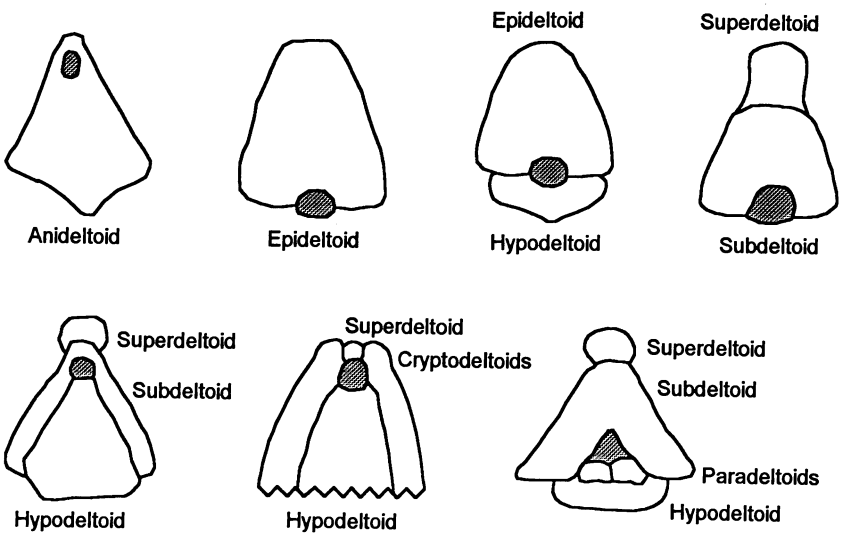

FIG. 1—Schematic arrangement of currently recognized combinations of anal deltoids. These may be further differentiated by presence or absence of hydrospire slits and exposure or concealment of plates below thecal surface. Anal opening is shaded. After Beaver, Fay, and Moore (1967).

ontogenetic variation, although if several specimens were available, character states on the largest and presumably most ontogenetically advanced specimen were coded whenever possible. Some states may be idiosyncratic for the individual specimens examined and may not necessarily represent all other members of the species or genus. A thorough analysis of variation would therefore be expected to change some codings in the data matrix (Table 2).

The specimens available for examination varied greatly in quality of preservation. Features that were liable to loss during preservation were coded conservatively, with the degree of preservation being assessed in part by the presence or absence of fine details such as growth lines or ambulacral grooves. When a feature sensitive to poor preservation was absent but other fine details on the specimen were observed, the absence was taken to be morphological rather than preservational. On the other hand, if no fine details were observable on the specimen, the specimen's character state was coded as unknown rather than absent.

In a few cases, where specimens were poorly preserved, observations were made on a second species of the same genus to code selected characters, the assumption being that both species share identical states at least for the particular characters being observed. No attempt, however, was made to represent the "essence" of a genus or to code generic concepts. Observations on actual specimens were supplemented by reference to published photographs, illustrations of thin sections, and written descriptions, although written descriptions were checked against specimens whenever possible. When a written species description was ambiguous or suspect regarding a particular character and could not be checked, the character was left uncoded. In keeping with this conservative approach, characters diagnostic of a genus or higher taxon were not assumed to be present in the particular species under study and were not coded unless positively reported. Interpretive drawings and reconstructions were also avoided when coding characters so as not to code illustrators' conceptions rather than actual features of specimens. The data matrix therefore consists largely of personal observations or well-documented, positive observations from the literature, although some existing gaps in the data matrix could be filled in if the assumption were made that characters in interpretive illustrations or familial and generic diagnoses are present in the species under study.

CHARACTER CODING

Table 2 presents the data matrix of 94 characters, with 153 possible character state transitions, used in this analysis. The characters and states are listed in the Appendix, with parenthetical notes providing additional information on the coding of particular characters. Since compilation of the data in Table 2 involves many fundamental decisions on morphological analysis and coding, and the data in Table 2 are the basis for the interpretation of blastoid phylogeny, it is appropriate to discuss some of the specific approaches taken in recognizing and coding characters. The following paragraphs use specific examples of blastoid character coding to illustrate a number of general coding considerations.

Ordering.—Most characters were treated as unordered, which in effect assumes that transitions are freely possible between all character states. Exceptions were character 65, which is part of a mixed binary coding with character 66, and characters where geometric intermediates were clearly present, as in characters 6, 11, 27, and the quantitative characters 87 through 91.

Some characters that appear to have ordering, such as those indicating the number of pores per side plate (characters 43 and 44), are left unordered because the apparent ordering does not reflect geometric necessity. That is, some species (such as *Granatocrinus granulatus*) show two pores per side plate along both the radials and deltoids. Others (such as *Cryptoblastus melo*) show two pores per side plate along the radials and no pores along the deltoids. The transition between these states (as by infilling of deltoid pores) does not require that every second pore be filled in first to yield a one pore per side plate condition before an absence of pores can be achieved.

Weighting.—Initially, all characters were given a weight of 1 (i.e., the phylogenetic analysis assigns each transition between character states equal weight). Equal weighting is reasonable for discrete characters since it implies that each evolutionary change is equivalent, whether changes occur in separate characters or between discrete states of a single character. The implications of equal weighting, however, are slightly less straightforward in continuous characters (Swofford and Begle, 1993). Since continuous characters can be divided into an arbitrary number of states, each state representing an evolutionary step, continuous characters can vary in their weight relative to other characters in the analysis. Continuous characters that are heavily subdivided have a greater potential to affect the outcome. One way to address this disparity is to give the entire series of transitions between character states a maximum weight of 1, so that a complete pass through all states will have the same influence as a binary character. This treatment permits the inclusion of data whose states may have overlapping or indistinct boundaries without over-emphasizing the demarcation of states. If, however, more than one evolutionary change is reflected in the continuous data, assigning a total weight of one to the character underrepresents the information content of the character. Scaling arbitrarily divided characters so that the sum of all transitions between states equals the weight of a binary character is therefore an extremely cautious way to address the uncertainty involved in recognizing discrete character states. For this analysis, states in continuous characters are determined by the location of gaps in the distribution of continuous measures, with the implication that these measures are clustered in natural groups or evolutionary states. While this assumption has not in fact been demonstrated to have merit, one of the corollaries to the assumption is that transitions between states are separate evolutionary events and should therefore be given the same weight as other character state changes. For comparison with the equal-weighting analysis, selectively weighted analyses were run in which continuous characters and other characters that admitted some arbitrariness in the recognition of states were deweighted to give a series of transitions through all states a total weight of 1 for each character.

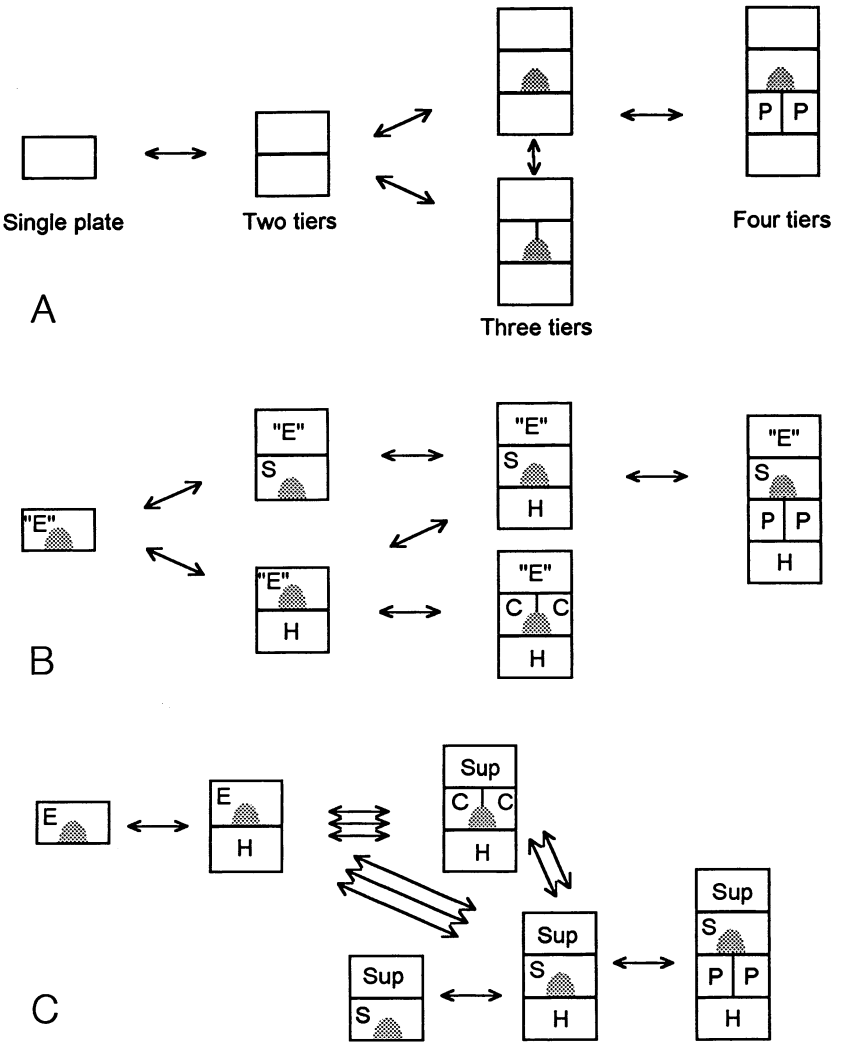

FIG. 2—Alternative characterizations of anal deltoid plates. Arrows indicate the number of evolutionary acquisitions or losses required for transitions between plate arrangements. Shaded area is anal opening. A, Plates specified by number of tiers, with homologies of individual plates in single-, two-, and three-tiered arrangements left unspecified. B, Superdeltoids homologized with epideltoids ("E"), but all other plates interpreted as distinct structures. C, Transitions under presence/absence coding using traditional plate names. Many transitions between configurations require more than one evolutionary step. Abbreviations: *C*, cryptodeltoid; *E*, epideltoid; *H*, hypodeltoid; *P*, paradeltoid; *S*, subdeltoid; *Sup*, superdeltoid.

Specific coding examples.—One of the most striking features of the character list is that spiracles and spiracular slits, both of which are important in current classifications of the blastoids, are not explicitly coded as characters. This is because spiracles and slits are not actually discrete structures in themselves, but rather are produced by particular arrangements of several separate structures. The presence of spiracles is indicated in the matrix by the combined states of having hydrospire slits concealed and having pores present (states 11.0 or 11.1 plus states 18.1 or 19.1). Likewise, the presence of spiracular slits may be inferred by

having hydrospire slits concealed but pores absent (states 11.0 or 11.1 plus states 18.0 and 19.0). Coding both the presence of spiracles and the degree of exposure of hydrospire slits would in effect give a single morphological condition double weight in the analysis.

Characters reflecting the number and the arrangement of anal deltoids provide additional examples in which familiar descriptions must be abandoned. The Treatise presents the current naming scheme for anal deltoid plates (Beaver, Fay, and Moore, 1967: S316), emended by removal of anideltoids as a separate plate configuration (Macurda, 1975) and recognition of a subdeltoid instead of cryptodeltoids in the *Polydeltoideus* configuration (Breimer and Macurda, 1972: fig. 1). The fact that plates that appear in different arrangements have been given a common name implies that the plates are homologous, but these homologies have been presented without justification. For example, the single plate in *Codaster acutus* is called an epideltoid, implying homology with the adoral-most plate in *Hyperoblastus filosus*. The most adoral plate in *Heteroschisma subtruncatum*, however, is called a superdeltoid even though it occupies the same relative position on the theca as does the epideltoid. Crystallographic data can help evaluate the status of various named anal deltoids (Bodenbender, 1996). In the present study, epideltoid and superdeltoid plates are considered homologous since they occupy similar positions as the most adoral of the anal deltoids and have *c* axis orientations that overlap extensively (Bodenbender, 1994: fig. 2.14.3, 1996). Homologizing these plates leads to a much simpler treatment of anal deltoids than that of the Treatise (Beaver, Fay, and Moore, 1967: S316).

For this study, the diverse configurations of anal deltoid plates in blastoids (Fig. 1) are summarized in two characters: the position of the anus relative to the deltoids (character 63) and a mixed binary character based on the number of anal deltoid plates (characters 65 and 66). Figure 2A illustrates the hypothesized character states and transitions between states. In this treatment of anal deltoids, evolutionary transitions between the single-plated and double-plated conditions (states 65.0 and 65.1) can only be considered homologous if the same plate is gained or lost with each transition. The coding, however, does not require that one specify whether the adoral or the aboral plate is the one involved in each transition. This is less assumption-laden than coding the presence or absence of named plates, which would require that the identity of all plates, including single ones, be known with certainty. Crystallographic data are ambiguous as to the identity of single anal deltoids (Bodenbender, 1994, 1996), but for this study the assumption that the same plate is gained or lost in each transition between single- and double-plated conditions is not particularly onerous since the single-plated condition occurs in only three taxa in the analysis. A parallel assumption, that homologous plates are gained or lost in all transitions between two- and three-plated conditions, is more problematic but is difficult to evaluate without additional developmental, morphological, or crystallographic data.

The coding of anal deltoids used in this analysis can be contrasted with one that more rigorously maintains the distinction between plates implied by their different names. Figure 2B represents transitions between anal deltoid conditions implied when epideltoids and superdeltoids are homologized on crystallographic grounds but all other named plates are recognized as distinct entities and coded by presence or absence. This coding differs from the mixed binary coding (Fig. 2A) in requiring two evolutionary steps for transitions between the two separate double-tiered configurations and between the two three-tiered configurations.

Among the differences between the two codings is the interpretation of subdeltoids and cryptodeltoids. The mixed binary coding, by focusing on the number of tiers of plates, reflects previous interpretations of subdeltoids and cryptodeltoids as fused and split variants, respectively, of a single morphological entity (Beaver, Fay, and Moore, 1967). The coding that uses presence or absence of plate names, however, treats cryptodeltoids and subdeltoids as separate, independently derived entities by requiring two steps for the transition between them. Few crystallographic data are available to aid in choosing between interpretations since subdeltoids have only been measured in two species so far. One of the two species supports each of the competing interpretations (Bodenbender, 1994: fig. 2.14.3, 1996), suggesting that

TABLE 2—Character matrix of blastoid morphological features. Characters are described in the Appendix. Ordering and weighting are discussed in text. *Stephanocrinus* spp. are outgroups. *Cordyloblastus* has been synonymized with *Hyperoblastus* (Breimer and Dop, 1975), but since data were mistakenly gathered on *Hyperoblastus filosus* and *Cordyloblastus eifelensis* as representatives of separate genera, both species are retained in this analysis. Use of the name *Cordyloblastus* is for ease of reference and does not imply anything about the taxonomic status of the genus. Data on *Macurdablastus*, gathered after analyses were completed, are included for future reference but were not used in any analyses reported here. Column labeled 'Strat.' is stratigraphic interval by zone (Fig. 7); stratigraphic ranges are ranges of genera, not of the individual species listed. Column labeled 'Alt.' shows alternative codings that reflect different interpretations of selected morphological features; alternative characters are included for comparison but were not used in final phylogenetic analyses. Symbols in table: dash (-), not applicable; space ( ), missing data.

	Standard coding ....*....1....*....2....*....3....*....4....*....5....*....6....*....7....*....8....*....9....	Strat. *	Alt. ....0....*.
Stephanocrinus angulatus	00100------ ---------10202001 0 02 ---0 -- -----010-000100001---001001001101 01010 10001	0	--000100001
Stephanocrinus gemniformis	10300------ ---------1 20200 0 02 ---0 -- -----010- 0 100001---001001001101 00-01 0101	0	--0001 001
Stephanocrinus hammeli	00300------ ---------1020200 0 02 ---0 -- -----010- 0010000 0010010011 1 00-1133010001	0	--0 00 0
Stephanocrinus osgoodensis	00300----------10202000 0 02 -- 0 -- -----01 - 001 00 0---00 00 00110 000-11 001	0	--000110000
Ambolostoma baileyi	10 213 110001- 001 10120120 2 100 110 112010 0001010000010 01000001 10 0- 1	12	1000 0
Angioblastus wanneri	100 13-10-2-0-00-00-200202000 11 000011011-- 1000100011000012001 1---0 0001001102 00-0132020222	14-19	00000011000
Anthoblastus stelliformis	115 13010 00 020100-0 020111 02 0000110 1--0 10 100100101001 1---000010001102 00-01 0 102	16-18	22000 11000
Arcuoblastus shumardi	106 13 1001-1 2010000 2230 10 1000010000111000000101000000001 21 01010000 102 01 0103202	9	22100001100
Astrocrinus tetragonus	110 12010300 020000-000 0230 1 110000 1 1-- 101 0001 000010010210-000 0020 0--2-0-31 12	12	11100 01100
Auloblastus clinei	105 13 113001- 011000222301 1111000 0 1121002000201000000011210001010001210 2 00-010300	9	100001100
Austroblastus whitehousei	151 -2- -20-00- 0 -- 100000111 1---0 00000	17	11 11000
Brachyschisma corrugatum	105 14010-2-1-21-00-00052210 0-112000100 --21002110111000 1001120--000000101102 01301 201 102	5-7	10000001001
Calycoblastus tricavatus	05 14 110001-201010000302 1 0101120011011012100000000100000000112110010000010110 100103001	17	22100001100
Caryoblastus bohemicus	104 13 10 001-20000-0 020 10100-112 0 0-- 10 0 00110100100 2110011100101100 0100122010000	5	12000101100
Codaster acutus	000 14-00-2-1-20-00-31051000 0101000001011--2110010101000001100000---000000001102 00-0132020222	11-12	11000010000
Cordyloblastus eifelensis	005 14001000 -100010000 02001 0011200010010111002000011010010010 20--011000101101 00-0122010000	5-8	22000101001
Costatoblastus sappingtonensis	10 13 01100 -100 10000 2220 01011 00110 11110020001010 0 0001 1---01010000 102001211 0	9	2100111000
Cribroblastus cornutus	1 6 12 112001-1020100002023 1010 1100 10 011101 000201001 1001 212001000000 110 120103002	11	22100001100
Cryptoblastus melo	106 12 11200 -10010-000102301 1011000110010211002000201000100011210-010100010100 0120103002212	9	2 100001100
Cryptoschisma schultzii	004 14-000000100-00-20121100101110000 1001--201020000100000100 021100 0000101102101003201 0020	5	00001101100
Decaschisma pulchellum	001 14 10 101-20-00-000 1100100-1020 10 --100020000110100100 20--010100001101 2100122010 20	2	11000101001
Decemoblastus melonoides	105 12 300 - 0201000 22 0 0 001200010 0101002000201000 000 12120000 0002 102 0120103002	9	2 100001100
Deliablastus cumberlandensis	1 0 12 300 -100010000102211 1 11000 10 1111010000201000 0001121 01000001 102 01351 0	10	22100001100
Deltoblastus permicus	106212 10300 - 1 10100301311021 0000110011111110100000100000100101---110000000100 00-0101202 13	19	110011000
Dentiblastus sirius	1 12 20 10001000 22 0 12 10 011000 0010 0 100101---02 01000 102 0100122012	9	22 0 11000
Devonoblastus whiteavesi	105 14 10000 - 0 1000 1222010101120011001012100000010101000001021 0-010100001102 0100103001102	7	100101100
Diploblastus glaber	115 120111001-10201000012220101011000110111111002000101010000011210-000100001112 0100113011211	12-13	22100101100
Elaeacrinus venustus	106112 113002- 1 1 00042230 00- 02000101 11100 0010100000001121100 010000 102 01 4100202	6-7	110001100
Eleutherocrinus cassedayi	105 14 110101-10001000012221100- 12000110 0121000000101000000001021100 010000-10-2-100103001102	6-7	22100001100
Ellipticoblastus ellipticus	106 110-10000-10010-000122301101110001101122000010001011110000011210-010100002100 0120102102212	10-11	22100001100
Euryoblastus veryi	11 12 030 1- 201 000 122 1 1100 0 11 0 201000 00011 010 000102 010 1	10	1001 1 00
Globoblastus norwoodi	116112 11000 -10010-000122301 10011000100 0210200000201100000011210-0101000101000120113012 23	9	22100001100
Granatocrinus granulatus	106 11 -13000- 0011000 102311 1 10001100 22 1000000201000 000111---00000001 10 1221 02	10-11	100011000

	Standard coding ····*····1····*····2····*····3····*····4····*····5····*····6····*····7····*····8····*····9····	Strat. *	Alt. ····0····*·
Hadroblastus whitei	115 14100-2-1-20-00-10052110101111100011100 --11202100011000010010 1---0 0100002102 0101122011202	9-12	111 0111000
Heteroblastus cumberlandi	106 1 3002- 1 1000 101311 0 001100 11 101001 100 02010000 1 1321 0	12	1100 1 00
Heteroschisma subtruncatum	001 14-11-101-00-00-00010200 0- 1200010 1--21000110010000010000 1---0 000001101 00-0122010022	6-7	00000000001
Hyperoblastus filosus	105 14011001 -10001000010220100- 12000101101110000001110100100 1020--011100001102 0100113001100	5-8	22100101001
Katoblastus konincki	101 14 0 2101120 00-30021 10101011000010 01--11100100101010000 01 2110020100001102 0100122010102	9	11000101100
Koryschisma elegans	101114 10 1 1120100-100 02101 10 1000110 --1110 101010 100111---01 10000 10200100112010	9-13	00011000
Leptoschisma lorae	001 14 11 101- 0-00-00020200100-01200 10 --10002000011000010 020--011100001101 0100122010	4-5	12000101001
Lophoblastus inopinatus	105 13 10200 - 1 10100 12201010100001100111100110002010000000111---000100001100 0100102001213	9	100011000
Macurdablastus uniplicatus	0 11 -0 1 0 1 1 000 1 0 0100000100 0 1000000101 00-01 0	1	00
Mesoblastus crenulatus	100 13 103001- 011030012220 01011000110110001100000101000000002110010 00002102 0101113002213	9-11	100001100
Metablastus wortheni	01 14 00100 20101001030010100 120001000 11100000001101001001 2110010100001101 1100112010120	9-11	1 000001100
Monadoblastus granulosus	106 11 - 300 - 0 1000012230101 10000101102010020000010001000111---0 010000 10 120113002 11	9	100011000
Monoschizoblastus rofei	106 11 -12002- 010-000222301 10100001100102112010000010000000111---020100000100000120101202 12	12	110011000
Montanablastus baldyensis	101 13 00 1 00010000 1 10 1 1 001100 11 11 1010 0 000 1---0001000011020 01	9	00011000
Nannoblastus pyramidatus	113 11--0-2-0-00-00-21 20 000 2 01 0 1--11 0 00100000201 1---000101001101 0100022020101	16-19	00000011000
Notoblastus stellaris	14 00-2- -20-00-30 422 0001 1 000110 1--2100000011 0000111 0 1000 102 01221	17-19	110 0 0
Nucleocrinus meloniformis	106012 113002- 1 10000422300 0-10200010 11100120001010 0 0001121110 01000011020 1 4100202211	6-7	110001100
Orbiblastus hoskynae	106 13 200 -10101000 21231 10010000100 11110000001010000001 1---010 00011100 01 0102102	9	22100011000
Orbitremites derbiensis	116 111-10002-10011000022230111010001101 11102010001011100001 1---02010000 100 0122102202212	12-19	22110011000
Orophocrinus stelliformis	004114010300 010100-00052000 01 1000 0 --21 12000011000000101---0 000010110200100122011102	9-12	22 00011000
Pentremites godoni	105214010000 -100 1 301210211020 10011100111201010001010000000111---010100000102 0100112101212	9-13	22100011000
Pentremitidea archiaci	004 14-01 101100-00-10020 00100-0120 0 --1100 00001100001001 2110011000011101 2130132010020	5	00001101100
Pentremoblastus conicus	101 14 0011-2000103001011010101100011001010110200011001010010 010100001101 01001 010020	9	11000101 0
Perittoblastus liratus	110 1 300 - 201 00 30230 1 110 0 111100 0 10101000001 010 00001112 01351 3 0	10	1000 1 00
Phaenoblastus caryophyllatus	001 14 002111120100-300200101010110001100 --1010000001 000 100 10010000001101 0100122010000	9	1110010 100
Phaenoschisma laeviculum	001 140110111120100-10020200101110000 1001--10102000010000010010 1---010000001101 100122010020	9-13	1 000 11000
Placoblastus ehlersi	106012 113002- 1 1 00042230 00 020 010011120 1 1010 0 00011211 0 010000 10 001 4100202	6-7	110001100
Pleuroschisma lycorias	105 14 011101- 0-00-00010210100-11200-0000--21000000011000001001 211 01100010110100100122010122	5-7	11000101100
Polydeltoideus enodatus	001 140011100-20-00-11020000 00-012100100 --10000000110000100103O--0 100000 10100100132010020	3	11001101011
Poroblastus granulosus	106 11 -13000-100110000122301 10110000101 12112000001010001000111---010100001100 010010 02 11	9-10	22100011000
Pterotoblastus gracilis	015113- -2-0-00-00-01002201002- 110 110 1--0100 00001000001200000---000010001102 0-0122020102	17-19	00000010000
Ptychoblastus pustulosus	1 6 11 -1300 - 01 0001123 1011 100001001 2110 010100010001 1---00010000 10 01201 0	9	10 011000
Schizoblastus sayi	116112 013002-10101100011230 10 00000100 01201110002010001000111---020 00001100 0130101202211	9	22110011000
Schizotremites kopfi	101 14 011001-100010000 0211100- 12000100 11100 0001010010100 210 010100001101 1001 0	7	22100101100
Strongyloblastus petalus	1052140012001-101010300312211010 10001100101201000001010000000111---010100001102 01001 0 202	9	22100011000
Tanaoblastus roemeri	100 12 11300 -10011000011220101011000110110101000000101000100010210-010100001102 0122112001202	9	22100001100
Timoroblastus coronatus	12 110-1-2-1-10-00-200202001 11 0100110 1--21 0000001000001101 1---01000 20-102 012 133120222	19	22000011000
Tricoelocrinus woodmani	100 13 1 100 - 1010010200101 0- 12000100 11110000000110000100 21 0100000011010110000 30 1 22	10-11	100001100
Troosticrinus reinwardti	001 14010100 -200010100200001 0- 120 -00 0111002 01100001001021 01100000110 00-0122010020	2	11000101100

neither treatment of subdeltoids and cryptodeltoids may be universally applicable in blastoids. The coding implying homology of cryptodeltoids and subdeltoids (characters 65 and 66) is favored here because of positional and structural similarities between these plates, but their homology is not certain. The alternative coding of Figure 2B (characters 102-106) is analyzed to evaluate the impact of the interpretation of homology.

An uncritical coding that utilizes all traditional names for posterior deltoids implies an even more strongly structured set of evolutionary transitions between anal deltoid configurations (Fig. 2C). Transitions between some states would require the loss of all plates and gain of entirely new ones in an unparsimonious series of evolutionary steps. The coding of all plate names is not considered here because of the highly-weighted evolutionary transitions it implies. Even if one were to accept the homologies (and consequent character state transitions) implied by the traditional names of posterior deltoids, an unmodified coding of these names introduces double weighting of transitions between states. For instance, presence of a superdeltoid can be inferred from the presence of cryptodeltoids or a subdeltoid. Each time cryptodeltoids or a subdeltoid are gained or lost, a superdeltoid is as well, so the superdeltoid should not be coded as an independent character. Doing so counts an additional evolutionary step for each transition between configurations that have a subdeltoid or cryptodeltoids and configurations that lack them. Such transitions will therefore be favored less often in a parsimony-based cladistic analysis.

Other characters associated with the anal deltoid plates may also introduce double weighting of character-state transitions, at least when viewed in terms of a particular hypothesis of character evolution. Consider the hypothesis that the transition to the single-plated condition is the result of the loss of a hypodeltoid. The combination of the location of the anal opening (character 63) and the portion of the additive binary coding of anal deltoids that reflects the number of plates (character 65) would yield a weight of two for the hypothesized single evolutionary transition because both the number of plates and the location of the anal opening would change when a hypodeltoid was lost or gained (see Fig. 1). To get a weight of one, the location of the anal opening would have to be coded as uncertain for single plates. Such a coding scheme is not used in this study because the initial identification of the missing plate as a hypodeltoid in individual specimens is not firmly established. This example, though, shows that coding schemes by default weigh against some interpretations while favoring others. The coding of anal deltoids implemented here favors the interpretation that the same (unspecified) plate is gained or lost in different transitions between the states of Figure 2A.

The coding of the two sets of hydrospire folds in the posterior interarea (characters 15 and 16) provides another example of how choices involved in converting morphology into characters can potentially affect the analysis. Posterior hydrospire folds may be present in full number, present but reduced in number, or entirely absent, and in addition folds may be differentially reduced in number on one side of the interarea relative to folds on the opposite side. Alternative schemes for coding the folds imply different weights for character transitions. Coding the configuration of hydrospire folds on each side of the posterior interray independently from the condition on its counterpart (characters 96 and 97) accurately records in the data matrix the actual observations made on specimens. This approach, however, gives the transition from no folds present on a specimen to some folds present on each side of the posterior interarea a weight of two (one step for each side of the interarea), whereas one can conceive of mechanisms effecting this change in a single evolutionary event. A different approach that codes the two sides of the interarea as a set (characters 15 and 16) masks some bilateral variation in the number of folds since if folds are present in full number on at least one side, whether they are reduced in number or not on the other side, the set is coded as having the full number. This coding also requires the assumption that symmetry in the distribution of hydrospire folds is homologous whether that symmetry is produced by the absence of all anal area hydrospire folds or the presence of folds on both sides of the interarea. For the taxa included in this analysis character 16 is uninformative, negating the need for an

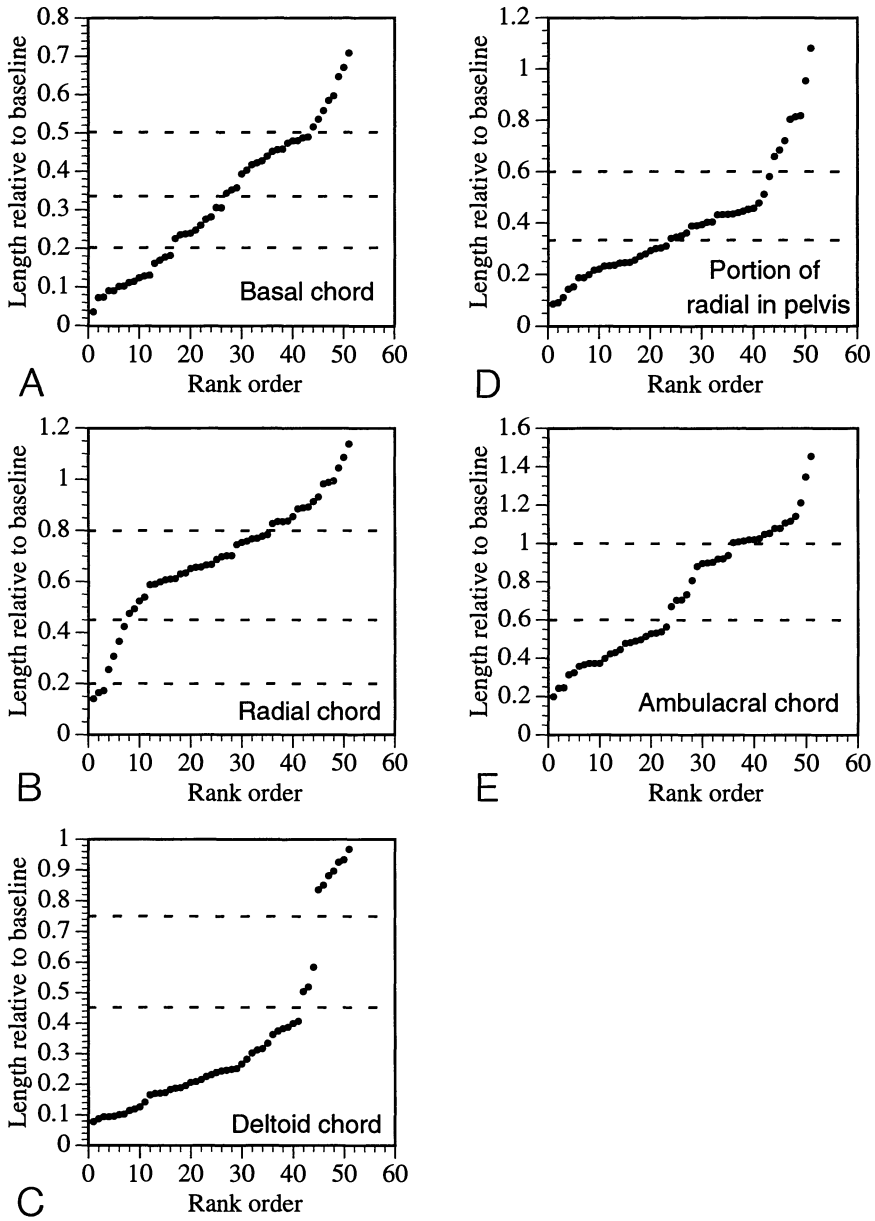

FIG. 3—Gap coding of continuously-varying character data. Lengths, ordered from smallest to largest, are distances between landmarks standardized relative to a baseline of unit length for each specimen. Size of gaps along vertical axis, rather than slope of line, is important in assessing character states. Dashed lines are boundaries between character states. A-E, Subdivisions of characters 87-91, respectively.

assumption of homology between symmetrical conditions. It is likely that the variation masked by character 15 is relatively uninformative as well, given the observed variability in fold number among regular deltoid interareas. The coding of characters 15 and 16 is therefore pref-

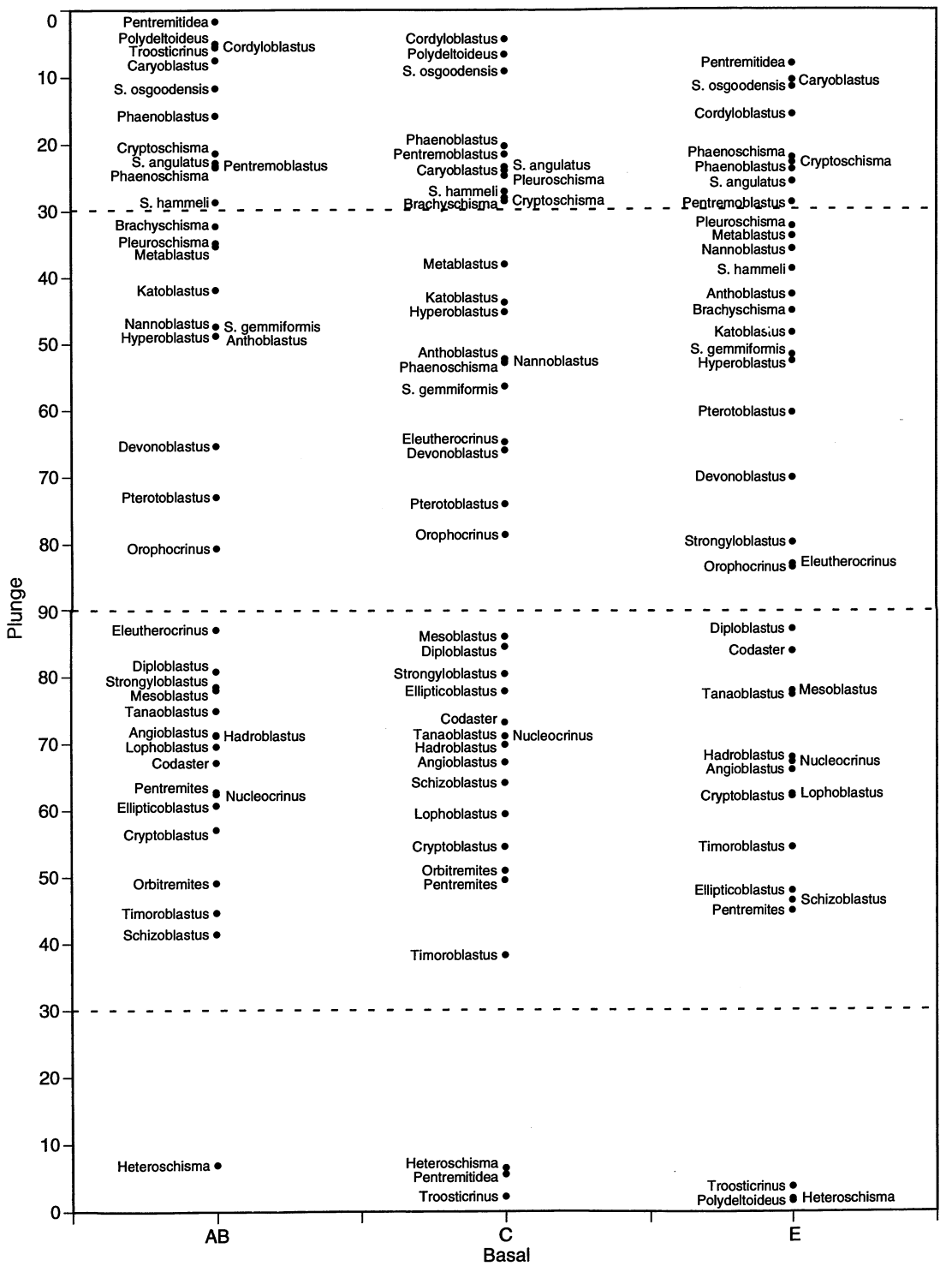

FIG. 4—Division of basal plate *c* axes into character states (see Appendix, character 92). Plunges of axes are plotted relative to plates oriented with their abaxial surfaces facing the top of the diagram. ⇒

erable to the double weighting implicit in coding each side of the ambulacrum separately as in characters 96 and 97. For comparison, both codings are examined in separate analyses.

Cladistic analysis proceeds on the assumption of independence of characters. In order to satisfy this assumption, characters representing features that are necessarily correlated, such as the spiracles or superdeltoids mentioned above, must be avoided. Some characters, however, are partially correlated yet have the potential to contribute some independent information to the analysis. Such characters have been retained in this study. An example is the location of the ambulacral tips and the length of the ambulacrum (characters 27 and 91). The first records the height of the lateral projection of the ambulacral tip onto the oral-aboral axis, while the second is a measure of the linear distance from the oral surface to the ambulacral tip. In many species, both of these characters will reflect the presence of long ambulacra extending to the base of the theca. In a few species, however, long ambulacra are supported on extensions of the radials rather than wrapped around the theca, so the two characters differ in their coding and present some independent information.

Blastoids show a wide range of variation in the shapes of thecae and various thecal surfaces. Unfortunately, in order to compare shapes and conduct the cladistic analysis, this variation must be parceled into discrete shape classes. Examples of this can be seen in the shape of the pelvis in lateral profile, the shape of the ambulacral outline, and the shape of ambulacral sinus walls (characters 3, 21, and 24). Specimens can be found that exemplify each of the classes recognized as distinct character states, but other specimens have more intermediate shapes. The coding of intermediates is open to subjectivity, for example in deciding how straight a thecal outline has to be in order to be coded as straight (character 3.1). While no definite rules can be formulated for placing intermediate shapes, conditions observed in repeated structures around the theca in some instances can serve as a guide for coding. For example, if an ambulacral sinus wall were nearly straight but slightly concave, the specimen would be coded concave if all other sinuses showed as much or more concavity, but would be coded straight if other sinus walls were straight or very slightly convex.

Continuous characters.—Foote (1991, and unpublished data) has digitized a series of landmarks on blastoid thecae. These landmarks can be converted into length measures approximating various dimensions of thecal plates that have been used in previous studies of blastoid phylogeny. The conversion of landmarks to length measures loses valuable information inherent in the relative positions of landmarks, and in some cases should be eschewed in favor of more sophisticated techniques (e.g., Swiderski et al., 1993). Lengths do have the advantage, however, of often being measurable on poorly preserved specimens not suitable for complete landmark digitization.

Landmark data are available for 50 blastoid genera, and for the outgroup species *Stephanocrinus hammeli* (Foote, 1991, and unpublished data). Distances between landmarks can be used to estimate the extent of the basals, radials, deltoids, and ambulacra, and can also estimate the length of the portion of the radial that forms the pelvis in the theca (see Appendix, characters 87-91). Length estimates calculated from the landmark data used here in many cases do not correspond exactly to standard length measures familiar to morphologists, for three reasons. First, all distances between landmarks are relative distances since landmarks from each specimen have been scaled to have a common baseline of unit length (Foote, 1991). The baseline is approximately equivalent to the oral-aboral axis. Differences in a given measure can therefore reflect absolute differences in the lengths of the plate under study, differences in length of the oral-aboral axis between species, or both. A second difference between the quantitative data used here and typical length measures is that many landmarks in this study are

---

Diploblastus plotted with A basal in AB column, C basal in C column, and DE (azygous) basal in E column. Dashed lines at 30° abaxial plunge, 90° plunge, and 30° adaxial plunge are boundaries between character states.

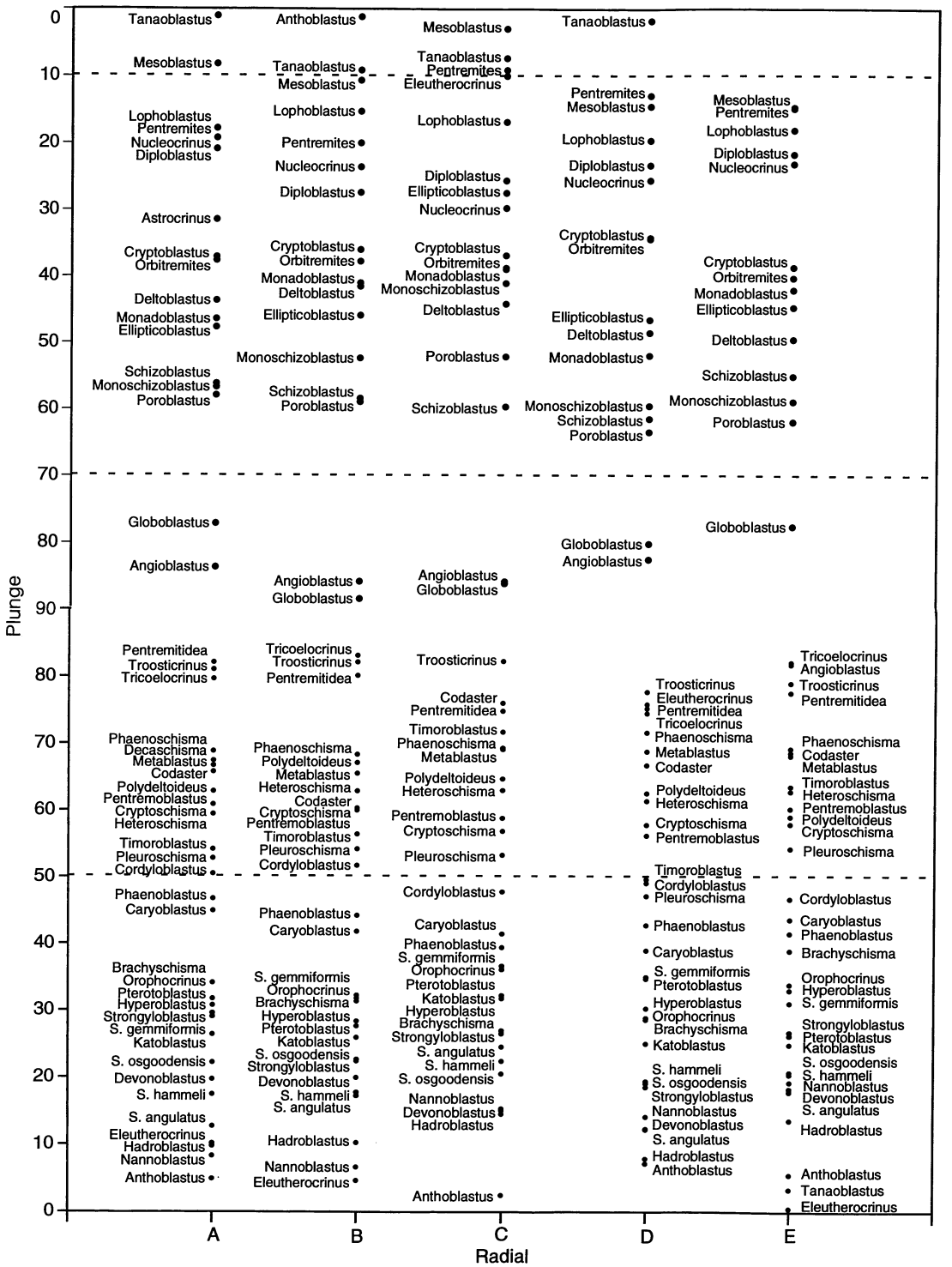

FIG. 5—Division of radial plate *c* axes into character states (see Appendix, character 93). Plunges of axes are plotted relative to plates oriented with their abaxial surfaces facing the top of the dia- ⇒

located at triple-junctions between plates. Depending on the species, these may or may not correspond to the extremity of a plate so the measures presented here are lengths between suture intersections rather than lengths between extreme points. Lastly, the calculated distances are lengths of chords connecting points directly rather than lengths measured along thecal surfaces or projected onto the oral-aboral axis. The landmark-based chords are still perfectly good morphological measures and often correspond quite closely to typical length measures, but they must be interpreted with the above factors in mind.

Cladistic methods have not satisfactorily addressed division of continuously varying characters such as distances between landmarks into discrete states. Although no clearly justifiable approach has been developed for determining discrete states for continuous measures, it seems apparent that continuous characters contain some information useful for phylogenetic analyses. One approach is to subdivide the character *a priori* into equal subunits and code each specimen by the subdivision into which it falls. This is quite common, and in fact is the basis for much previous morphological work and for many of the characters coded in Table 2 (e.g., character 27). An alternative, gap coding, seeks natural groupings of continuous data, recognizing groups by gaps in the data distribution. If closely-related taxa have similar values for a continuous character, gap coding should group those values in a single character state. Gap coding was employed for the recognition of states in the landmark data. The number of gaps to choose as boundaries between states is an open question (just as is the number of equal subdivisions to choose in the *a priori* recognition of states). Large gaps, however, present themselves as potentially more meaningful subdividers of characters than arbitrary, equally distributed divisions. Unfortunately, the chords calculated from landmark data show fairly even distributions, with few large gaps (Fig. 3). The largest gaps present were used to subdivide characters, with further divisions placed at smaller gaps in some of the longer, more or less continuous stretches in the plots.

Crystallographic data.—Data on the orientations of crystallographic axes can supplement the more familiar morphological data of phylogenetic analyses (Bodenbender, 1994, 1996). Crystallographic axes in blastoids show little variation in trend across species, but plunges are highly variable (Bodenbender, 1993, 1994: figs. 2.14-2.16, 1996). *C* axes in radial plates are generally oriented normal to the origin, or first-formed portion, of the radial, but axes from deltoid and basal plates appear to be less tightly associated with the orientations of the plates from which they are derived (Bodenbender, ms.). The orientation of the origin of the radial plate is not a character otherwise considered in the analyses presented here, so *c* axis orientations of blastoid skeletal elements do not duplicate existing morphological characters.

Crystallographic axis orientations are available for basal, radial, and deltoid plates from representatives of 43 blastoid species and all four outgroup species. These orientations vary more or less continuously, so their inclusion in the cladistic analysis is subject to the usual travails attendant to coding continuous characters, as discussed above. In addition, intraspecific variation in crystallographic axis orientations was taken into consideration in developing crystallographic characters.

Previous work has shown that crystallographic axis orientations in the three types of thecal plates may be quite consistent within a given specimen, but homologous plates from different specimens of the same species can have axis orientations that vary by nearly 60° (Bodenbender, 1994: fig. 2.5, 1996). Such great intraspecific variation places constraints on the number of states into which continuous characters such as crystallographic axis orientations should be divided. Since this study considers lower-hemisphere projections of *c* axes, axes can effectively vary though 180°. The 60° intraspecific variation suggests that the variability in axis orientations should be divided into no more than 3 states. In order to choose more states, one

---

gram. Dashed lines at 10° abaxial plunge, 70° abaxial plunge, and 50° adaxial plunge are boundaries between character states.

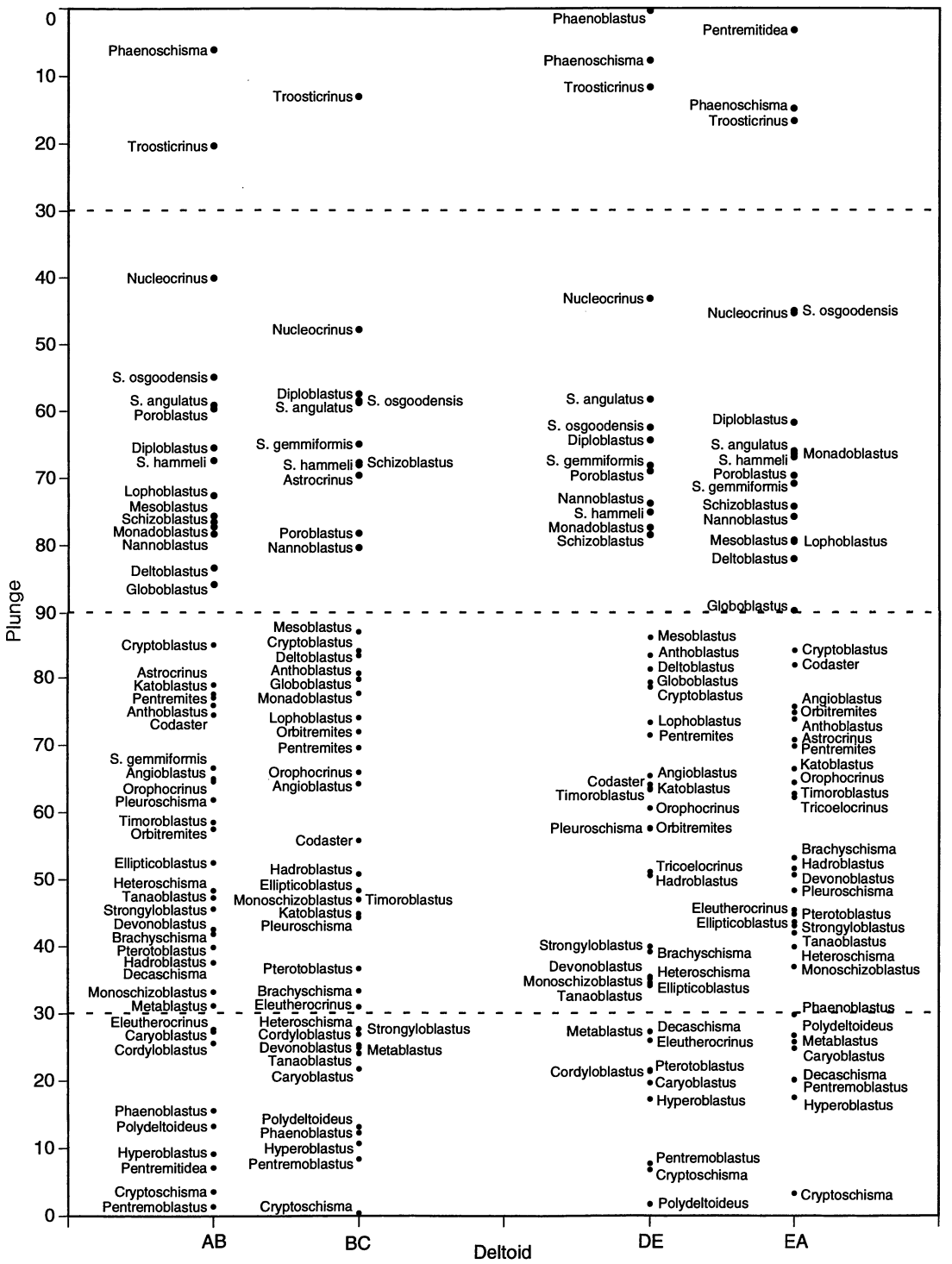

FIG. 6—Division of deltoid plate *c* axes into character states (see Appendix, character 94). Plates are plotted as though oriented with their abaxial surfaces facing the top of the diagram. Dashed lines ⇒

could measure multiple specimens from each species and code species averages for axis orientations. Species averages would be expected to vary far less than do individual observations on specimens. Limitations of specimens and time, however, dictated the use of single specimens to represent axis orientations for an entire species. Representing species with single specimens and recognizing a large number of character states would require an uncomfortable assumption that all observed specimens have axis orientations close to the mean for their species. Making this assumption risks improperly coding specimens that fall far from their species' average. Recognizing a maximum of three states for each crystallographic character is a more conservative approach that reduces this risk by accommodating more variation away from the mean within each state. Deltoids in some species, however, showed structured variation among *c* axes from the various interrays, with the AB and EA axes nearly vertical but directed abaxially and the BC and DE axes nearly vertical but directed axially (see Beaver, Fay, Macurda, Moore, and Wanner, [1967] for orientation terms). This specific pattern was detailed and distinct enough to be recognized as a fourth state.

Gap coding, with intraspecific variation restricting the number and spacing of gaps, was used to recognize boundaries between character states. In order to separate the observed crystallographic orientations into character states, *c* axes from all specimens were grouped according to plate type. Orientations of axes from the three basal plates served as the basis for one character (character 92), those from the five radial plates as another (character 93), and axis orientations from the four regular deltoid plates as a third (character 94). Anal deltoid *c* axes were not considered since anal deltoids are not homologous across all taxa. Within each character, trends of all axes from homologous plates (e.g., all AB basals or all A radials) were averaged using the computer program CalcAxes (Fisher and Bodenbender, 1993). Individual *c* axes were then rotated through an acute angle about the oral-aboral axis to the vertical plane containing the average trend for each plate type, thus maintaining their original plunges while aligning along a single, vertical great circle. The averages for the rotationally homologous plates of each type (e.g., averages of all A radials, averages of all B radials, etc.) were then rotated about the oral-aboral axis so that the average trends of all plates of each type coincided. This is akin to orienting all plates of a given type to face the same direction by rotating them to a common position on the blastoid theca. Alignment of all axes from rotationally homologous plates in a single plane facilitated the recognition of gaps in the distribution of plunges. The largest gap was marked as a potential boundary between states and additional gaps were sought at 60° intervals from the first. The axes within each interval were then examined to check whether axes derived from single specimens crossed boundaries between states (Figs. 4-6).

For basals and radials, the plunges of axes fell into fairly discrete groupings (Figs. 4 and 5). Gaps in plunges of basal plate *c* axes placed axes from 6 out of 40 specimens into two different states (Fig. 4). These six taxa were coded with the state occupied by two of the three axes. Each specimen had five radial plates and therefore contributed five axes to the plots of radial plate plunges, but in only 6 of 46 cases did axes from different radials on a single specimen occupy more than one state (Fig. 5). In four of these instances only one of the five radial axes occupied the second state. One of these axes was from the reduced D radial in the nonpentameral species *Eleutherocrinus cassedayi*. The lack of radial symmetry of this species accounts for its variation in axis orientations. Each of the four remaining species with a single wayward axis was coded with the state shared by its four co-occurring axes. The final two specimens had three axes in one state and two in another. These, too, were coded with the majority state.

The four regular deltoids were less clear-cut in their axis orientations. Axes from 13 of the 48 species with measurable deltoids crossed boundaries between states recognized on the basis

---

at 30° abaxial plunge, 90° plunge, and 30° adaxial plunge are boundaries between character states.

of gaps in the distribution of plunges (Fig. 6). Four of these species had axes plotting nearly vertically, and in each case axes from the EA and AB deltoids plunged abaxially while the axes from the BC and DE deltoids plunged axially. The boundary delimiting states could have been selected to place one or more of the four specimens fully into a single state, but because of the regularity in distribution of axes in these specimens they were coded as sharing a distinct state. Eight of the remaining nine taxa had three of the four deltoid axes plotting in the same state. These were coded with the majority state. The remaining taxon, *Eleutherocrinus cassedayi*, had two axes in each of two different states and was given the state into which the average orientation fell.

STRATIGRAPHIC DATA

Stratigraphic data for blastoids are derived largely from Waters' (1990) compilation of generic ranges, with each species assigned the range observed for the entire genus. Additional ranges have been drawn from Sprinkle and Gutschick (1990) or determined from information in Fay (1961b) with reference to COSUNA correlation charts (Childs, 1985; AAPG, 1985a,b, 1987). Ranges were initially compiled at the stage level, with the Visean further subdivided into three units (Waters, 1990). Concurrent range zones were then determined from the blastoid range chart, such that each species' first and last appearance coincided with a zone boundary (Fig. 7). Zones 3, 4, 14, 15, and 18 each combined two stages. No blastoid genera from the sample under consideration occurred in the Ashgill and Llandovery or the Famennian, so these stages were omitted rather than designated as separate zones. In the evaluation of alternative phylogenetic hypotheses by their correlation with stratigraphic occurrences of fossils, this is equivalent to specifying that hypothetical lineages can pass through the Ashgill and Llandovery or the Famennian without incurring a penalty for having no representation in the interval. The Llandeilo predates the earliest blastoids included in the sample under consideration and therefore has no blastoid representatives. This stage was designated as a zone, however, because the four outgroup species, by definition, share a common ancestor with all blastoids, this ancestor occurring in an interval before the earliest blastoid. In accordance with their status as proxies for the lineage that was ancestral to all blastoids, all outgroup species were assigned to this zone. While the earliest coronate echinoderms occur in the Llandeilo, *Stephanocrinus* does not appear until the Ashgill. Regardless of the outgroup's actual stratigraphic record, however, assignment of the outgroup to the zone preceding the first occurrence of the ingroup is generally appropriate since it reflects the assumptions used in designating species as members of the outgroup.

Species ranges were assigned with a range-through method, so some species are inferred to be present in zones where no actual representatives of the species have been found. With the exception of Zone 0, however, all recognized zones have at least one blastoid species actually present. The presence of blastoids in each zone is evidence that fossil preservation was possible during each interval. Absence from an interval therefore cannot automatically be attributed to poor preservation.

One particular range assignment should be clarified. *Cordyloblastus* occurs in the Devonian of Europe and has been synonymized with the American genus *Hyperoblastus* (Breimer and Dop, 1975), but the two are treated separately in this analysis (see Table 2). Both *Cordyloblastus* and *Hyperoblastus* were assigned the full range reported for *Hyperoblastus* (Waters, 1990).

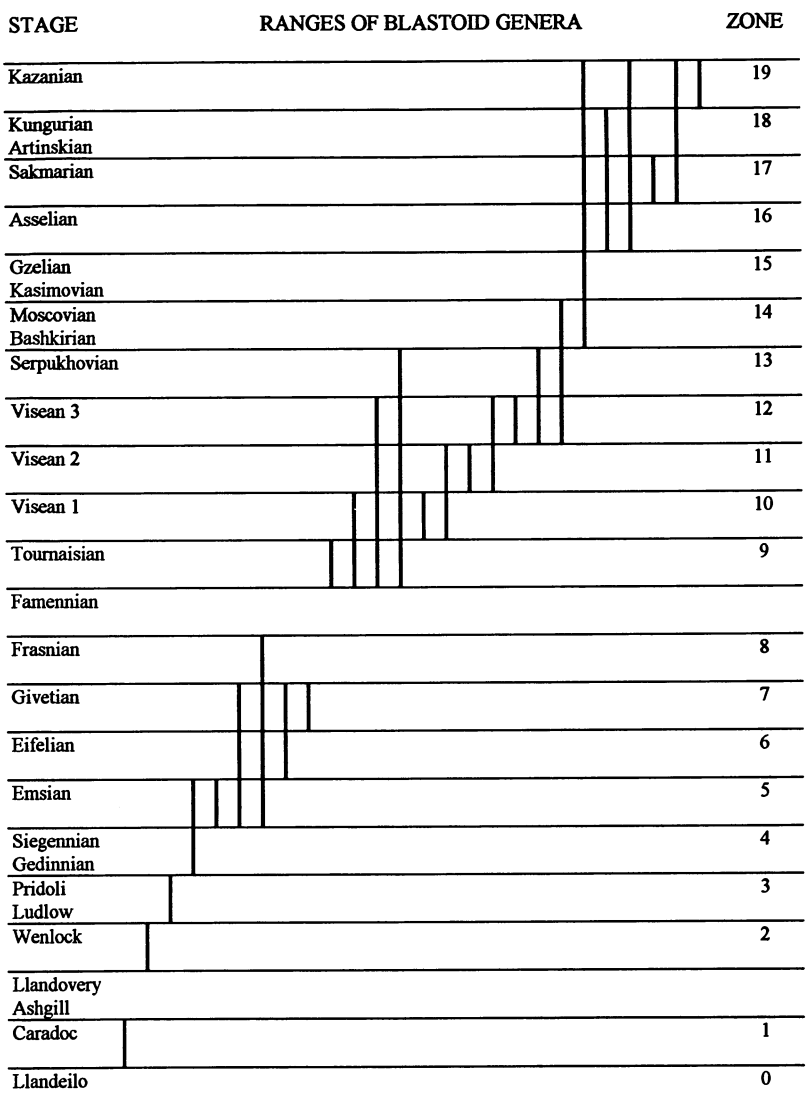

FIG. 7—Stratigraphic intervals recognized in the analysis. Numbered intervals are concurrent range zones based on ranges of blastoid genera compiled primarily at stage level (Waters, 1990). Vertical lines represent the 26 unique stratigraphic distributions displayed by the 68 blastoid taxa in Table 1. Ranges of individual genera are given in Table 2, character 95.

STRATEGY FOR ANALYSES

Cladistic analysis involves construction of alternative cladograms, searching for those phylogenetic hypotheses that are most parsimonious given the morphological data at hand. That

TABLE 3—Limited sample of taxa for exploration of alternative character codings using exhaustive search algorithms. Taxa represent major blastoid families recognized in Macurda (1983) and Waters and Horowitz (1993). Character codings for each species are given in Table 2.

Species	Family
Stephanocrinus gemmiformis	Outgroup
Brachyschisma corrugatum	Orophocrinidae
Codaster acutus	Codasteridae
Cryptoblastus melo	Granatocrinidae
Diploblastus glaber	Diploblastidae
Globoblastus norwoodi	Orbitremitidae
Hadroblastus whitei	Neoschismatidae
Heteroschisma subtruncatum	Phaenoschismatidae
Hyperoblastus filosus	Hyperoblastidae
Lophoblastus inopinatus	Schizoblastidae
Nucleocrinus meloniformis	Nucleocrinidae
Pentremites godoni	Pentremitidae
Polydeltoideus enodatus	Phaenoschismatidae
Troosticrinus reinwardti	Troosticrinidae

is, the hypothesis that requires the fewest evolutionary events in order to explain the distribution of characters among the taxa under study is the preferred hypothesis. Since the preferred phylogeny depends on the exact treatment of the data, several analyses were run to explore alternative coding schemes. Analyses were performed using PAUP v. 3.1.1 (Swofford, 1993). Current computer algorithms for cladistic analysis allow two types of search for most-parsimonious cladograms. The first is an exact search, where all possible combinations of taxa are evaluated, and the resulting cladogram or set of cladograms is certain to be the most parsimonious arrangement of taxa for the given character coding and assumptions. Complete evaluations of cladistic data sets with incongruent characters or moderate amounts of missing data are only possible for relatively small numbers of taxa because the number of permutations into which taxa can be arranged increases exponentially as taxa are added. For large data sets, such as the one examined here, the number of permutations to be evaluated outstrips currently available computing resources.

When the phylogenetic problem is too large for exact methods, heuristic methods must be used instead. Heuristic methods build an initial cladogram or set of cladograms based on an evaluation of characters that guides the placement of taxa as each is in turn added to the branching diagram. The initial cladogram or cladograms can then be rearranged in a search for more parsimonious arrangements. The set of shortest cladograms in a heuristic search may represent a local minimum for cladograms topologically similar to the starting cladogram, but the local minimum may or may not be the global minimum for the data set. Heuristic searches that evaluate identical data sets but start with different initial cladograms commonly find different sets of locally minimal cladograms. Each heuristic analysis presented here therefore conducted 10 repeated searches (using the TBR procedure in PAUP 3.1.1) from randomly determined initial arrangements of taxa and selected the shortest set or sets of locally minimal cladograms as the best available hypotheses of relationships, with the understanding that some still more parsimonious cladograms may remain undetected.

Repeated searches from random initial cladograms make comparisons between character codings problematic because the cladograms found in two completely random searches of alternative data sets could easily reflect the finding of different local minima rather than the influence of alternative coding schemes. A partial remedy that may promote the finding of cladograms from the same local minimum for use in comparing different character codings is

to use the same initial cladograms for the two searches to be compared. PAUP 3.1.1 has a pseudo-random number generator that will produce the same series of random numbers each time a given starting seed is used. Two searches run with the same seed, however, may or may not produce identical initial cladograms because the randomization only determines the order in which taxa are added during construction of the initial cladograms. Differences in the two codings may cause taxa to be joined to the cladograms in different places even though they are added in the same order.

Even if they start with the same cladogram, the two searches may wander to different local minima from their common starting point. This might be viewed as a property of the different codings, although it might more properly be considered a property of the search algorithm or its interaction with the data. An alternative to using the same initial cladograms, which may be far from the final local minimum, is to use the minimal cladograms from one coding of the data as the starting cladograms for the examination of the alternative coding. Unfortunately, neither Hennig86 (Farris, 1988) nor PAUP 3.1.1 properly implements a routine to search all of an initial set of cladograms. The first cladogram in the set is searched, but if the search yields a shorter cladogram the remaining initial cladograms are abandoned. Therefore, when a search in the analysis yielded multiple equally parsimonious cladograms, the first cladogram was used as a representative of the local minimum. In this way both searches will have at least visited the same minimal (for one data set) configuration, and different results will be partly attributable to differences in data rather than entirely attributable to the search algorithm.

The two procedures, searching cladograms produced by adding taxa in the same sequence and searching minimal cladograms from a competing coding, can find different local minima so the shortest local minimum observed for each data set is used in comparisons of coding schemes.

Two different sets of comparisons are presented. The first examines the effects of individual character coding decisions on the resulting most-parsimonious cladogram or cladograms. For these comparisons, a particular set of coding decisions is chosen as a standard coding (Table 2), then individual characters are varied from the standard according to alternative coding schemes. The effects of three particular character codings, each of which is discussed above, are examined. These are the treatment of the posterior hydrospires (characters 15 and 16 versus 96 and 97); gap coding of continuously varying characters compared with discrete states selected *a priori* (characters 87-91 versus 98-101); and the coding of anal deltoids as a series of hypothesized evolutionary transformations based on plate geometry (characters 65 and 66; Fig. 2A) versus coding by name (characters 102-106; Fig. 2B). A second set of comparisons examines two more general treatments of the data. These are the deweighting of all characters with arbitrarily divided or subjective states and the inclusion of crystallographic data.

Comparisons of individual coding decisions are explored with two different sets of taxa. The first is a set of 14 taxa consisting of one outgroup species and 13 well-studied blastoid species, representing 12 different blastoid families (Table 3). This limited data set can be analyzed with exhaustive searches, so the results are sure to report all minimal-length cladograms for each coding variation examined. The limited data set includes taxa from a variety of families to ensure that character states for all of the different character codings to be compared are adequately represented in the matrix. Using members of a single family to investigate alternative coding schemes, while perhaps more phylogenetically meaningful than the comparison of widely-separated taxa presented here, would not have permitted examination of all alternative codings. The full data set of 71 taxa (Table 2) is the second set of taxa within which individual character codings are compared.

For the full data set search times under equal weighting prohibited comparisons of codings parallel to the comparisons made using family representatives (Table 3). Alternative codings could be compared for the full complement of taxa if selective deweighting of characters was used since this treatment of the data happened to yield a relatively small number of equally parsimonious cladograms within an acceptable time frame. The standard matrix used for

TABLE 4—Alternative character weights used to selectively deweight subjectively divided characters. Analyses that apply these weights to each transition between character states are compared with analyses that use the preferred equal weighting scheme (see Figs. 8, 13-16, and accompanying text).

Char.	Wgt.	Char.	Wgt.	Char.	Wgt.	Char.	Wgt.	Char.	Wgt.	Char.	Wgt.	Char.	Wgt.
1	12	17	12	33	12	49	6	65	12	81	12	97	6
2	12	18	12	34	12	50	12	66	12	82	12	98	12
3	2	19	12	35	6	51	12	67	12	83	12	99	12
4	12	20	12	36	12	52	12	68	12	84	12	100	12
5	12	21	4	37	12	53	12	69	12	85	12	101	12
6	3	22	12	38	12	54	12	70	6	86	12	102	12
7	12	23	12	39	12	55	12	71	12	87	4	103	12
8	12	24	12	40	12	56	12	72	12	88	4	104	12
9	12	25	6	41	12	57	12	73	12	89	6	105	12
10	4	26	6	42	12	58	12	74	12	90	6	106	12
11	6	27	4	43	12	59	12	75	12	91	6		
12	12	28	12	44	12	60	12	76	12	92	6		
13	6	29	12	45	6	61	6	77	6	93	6		
14	12	30	12	46	12	62	12	78	12	94	4		
15	6	31	6	47	12	63	12	79	12	95	12		
16	12	32	12	48	12	64	12	80	12	96	6		

comparisons of individual coding decisions therefore used character weights as listed in Table 4.

Equal weighting of the full matrix produces results that differ from selective weighting. Rather than choosing the preferred outcome after results are obtained, the choice of which to accept should be based on the merits of the alternative weighting schemes. While deweighting characters that are subject to arbitrary subdivisions may be a conservative approach that lets an evaluation of a character's trustworthiness influence its weight in the analysis, the setting of the entire transition series to unit weight dismisses much of its potential to provide evolutionary information. In at least some multistate characters, even arbitrarily divided ones, the different states in fact *are* products of different evolutionary events, so passing among all such states would require more than the single evolutionary transition implied by scaling the character to unit weight. Equal weighting of all transitions between character states is more consistent with the assumptions made in recognizing the states as distinct in the first place. The cladograms found under an equal weighting scheme are therefore favored *a priori* in this analysis.

Analyses can also be judged *a posteriori*, although not solely on the basis of cladogram topology, if additional data can be consulted to aid in choosing among results. Paleobiogeography is one source of data that might be useful for evaluating competing hypotheses, but problems of incomplete preservation and sampling of strata, the long time interval spanned by blastoids, and uncertainties in Paleozoic continental reconstructions make this somewhat difficult to apply to blastoids. Data on the stratigraphic order of occurrence of fossils are obvious alternative criteria to use in deciding which analysis to favor. This *a posteriori* application of stratigraphic data is not a stratocladistic analysis *per se* since stratocladistics employs stratigraphic data during the analysis to build phylogenetic trees and chooses among alternative trees using a global parsimony criterion. Instead, the use of stratigraphic data discussed here is a sorting procedure that evaluates alternatives, originating from an analysis of morphological data alone, using information that was not included in the initial analysis. Stratigraphy can be useful both in comparing different analyses and in sorting among alternative

equally parsimonious cladograms from a single analysis (Suter, 1993, 1994). Assessment of the compatibility of phylogenetic hypotheses with the stratigraphic record follows the basic logic of stratocladistics (Fisher, 1982, 1988, 1991, 1992, 1994b). The gist of this logic is that cladograms with sister-group relationships that require few lineage segments to cross stratigraphic intervals without fossil representation are considered more compatible with the stratigraphic record than cladograms that imply many unrepresented lineage segments.

The number of instances in which lineages cross stratigraphic intervals without fossil representation is referred to as a hypothesis' stratigraphic parsimony debt (Fisher, 1982, 1992, 1994a). The analysis producing the phylogenetic hypothesis with lowest stratigraphic parsimony debt is most compatible with stratigraphy. Stratigraphic parsimony debt is discussed more fully by Fisher (1982, 1992, 1994a) and Bodenbender (1994).

Both alternative character coding schemes and alternative weighting schemes yielded multiple cladograms. These were evaluated to find the cladograms most compatible with stratigraphy in the results of comparative analyses, thus reducing the number of morphologically equally-parsimonious cladograms that issued from each analysis. The most stratigraphically compatible cladograms from the competing analyses were then compared with one another to determine which results were most compatible with stratigraphy overall. Parsimony, as expressed by tree length, cannot be used to compare analyses in which character weights, character number, or number of character states differ, leaving congruence with the stratigraphic record as the best available criterion for evaluating alternative treatments of the data.

RESULTS

Exhaustive analysis of selected taxa.—Exact (Branch and Bound) cladistic analyses of the 14-taxon data set (Table 3) show that alternative codings of individual characters have variable effects on the most-parsimonious arrangement of taxa. The characters under the Standard Coding heading in Table 2, less crystallographic characters 92-94, are used as a basis against which alternative codings can be compared. This coding with equal character weighting yields 38 equally-parsimonious cladograms that produce the strict consensus of Fig. 8A. The comparative analysis that examined the alternative coding of posterior hydrospire folds (substituting characters 96 and 97 for 15 and 16), found an identical set of 38 cladograms. The alternative coding of anal deltoid plates (substituting characters 102-106 for 65 and 66) achieves greater resolution, yielding two equally-parsimonious cladograms (Fig. 8B), both of which are among the 38 cladograms of the standard coding. Inclusion of crystallographic data (characters 92-94) yields 37 equally-parsimonious cladograms, 13 of which also match cladograms from the standard coding, with the remaining 24 representing different equally-supported hypotheses. The cladograms found when crystallographic data are included reduce to the same consensus as the standard coding (Fig. 8A). Similarly, dividing quantitative characters into states *a priori* instead of gap coding (substituting characters 98-101 for 87-91) results in six cladograms, three of which match standard coding cladograms. The consensus from this last analysis is compatible with the standard coding consensus but is somewhat more resolved (Fig. 8C).

The most striking aspect of these results is the lack of resolution with equal weighting under any coding scheme, especially given the relatively large ratio of characters to taxa. The poor resolution makes the detailed impact of individual coding decisions difficult to assess, although it can be said that more structured hypotheses of character change, such as that of the alternative coding of anal deltoid plates (Fig. 2B), appear to produce more structured results. Applying a selective weighting protocol (Table 4) rather than equal weighting also structures the results quite strongly, yielding a single, most-parsimonious arrangement that differs from those of the other alternatives and the standard coding by placing *Nucleocrinus* as the sister to *Lophoblastus* (Fig. 8D).

As previously noted, stratigraphic congruence can serve as a criterion by which to judge the alternative character coding and weighting schemes. The cladogram from the analysis of standard character codings (and from the identical results for the alternative coding of posterior hydrospire folds) that is most compatible with stratigraphy implies 22 instances in which lineages cross stratigraphic intervals without fossil representation. This cladogram therefore has a stratigraphic parsimony debt of 22. For the 14-taxon data set, stratigraphic parsimony debt resembles tree length in morphological characters in that its minimum value is not 0 but rather is a constant. Since the same taxa and stratigraphic coding are used in each data set, this constant applies across all analyses regardless of the coding or weighting of morphological characters. All alternative codings imply more than 22 unrepresented lineages. The stratigraphically most compatible cladogram from the analysis that includes crystallographic data has a stratigraphic parsimony debt of 23, while the minimum debt for a cladogram from the analysis of the *a priori* division of quantitative characters is 28 and from the alternative coding of anal deltoid characters is 35. All of these analyses employed equal weighting. While the analysis using selective weighting provided the greatest resolution, the single resulting cladogram is least compatible with the stratigraphic record, having a stratigraphic parsimony debt of 37, 15 units greater than the hypothesis from the standard coding. The results that include crystallographic data are not particularly incompatible with the stratigraphic record, but stratigraphic compatibility tends to favor the standard character codings over the other alternative character treatments, at least within this limited data set.

Generalizing the results of a small-scale analysis to a larger scale is difficult because characters can be expected to have different effects at different levels in a hierarchy of cladistic relationships. Some will be conservative only between closely related species while others may be conservative over several large clades. The distribution of character states in additional taxa may also restructure the data into patterns different from those evident in a smaller assemblage, for example when the new taxa represent plesiomorphic sister groups to other taxa in the analysis (Donoghue et al., 1989). Generalization is rendered still more difficult by the necessity of using heuristic rather than exact search methods in large data sets, so that any comparisons must be made with the assumption that the cladograms found in each analysis of the larger data set represent equivalent local minima if not the global minimum.

Heuristic analyses of alternative character codings.—Despite the reasons why an exact analysis limited to 14 taxa might potentially differ from a heuristic analysis of the full set of 71 taxa, results are in fact remarkably similar between the two data sets. The standard character codings for the full data set produce the consensus cladogram of Figure 9, which can again be compared to the results of analyses that incorporate alternative character codings. (Recall that comparative analyses using the full data set employ selective weighting, since equal weighting results in prohibitively long computer search times.) Replacing gap-coded quantitative characters (characters 87-91) with characters divided into states *a priori* (characters 98-101) does not affect relationships among basal taxa or the distal fissiculate clade (*Pentremoblastus* through *Pterotoblastus*). The alternative coding does, however, restructure the consensus to resolve placements between *Montanablastus*, *Orbiblastus*, and the *Strongylo-blastus* and *Lophoblastus* subclades, and alters the relative placement of several other spiraculate subclades (Fig. 10). The *Deliablastus* subclade is moved proximally relative to the other spiraculate subclades, while the *Globoblastus* subclade is moved distally. Along with the rearrangement of subclades, the *a priori* coding also reorganizes relationships within small groups of taxa, including *Mesoblastus* and *Tanaoblastus*, and *Ptychoblastus*, *Monadoblastus*, and *Poroblastus*. Inclusion of crystallographic data produces similar results, but with less resolution among the spiraculate subclades (Fig. 11). The *Deliablastus* subclade is again drawn proximally, and relationships between *Mesoblastus* and *Tanaoblastus*, and between *Ptycho-blastus*, *Monadoblastus*, and *Poroblastus* again differ from those in the standard coding. Coding anal deltoids by assuming the homology of named plates, as in Figure 2B, instead of emphasizing the number of tiers of plates as in Figure 2A (substituting characters 102-106 for

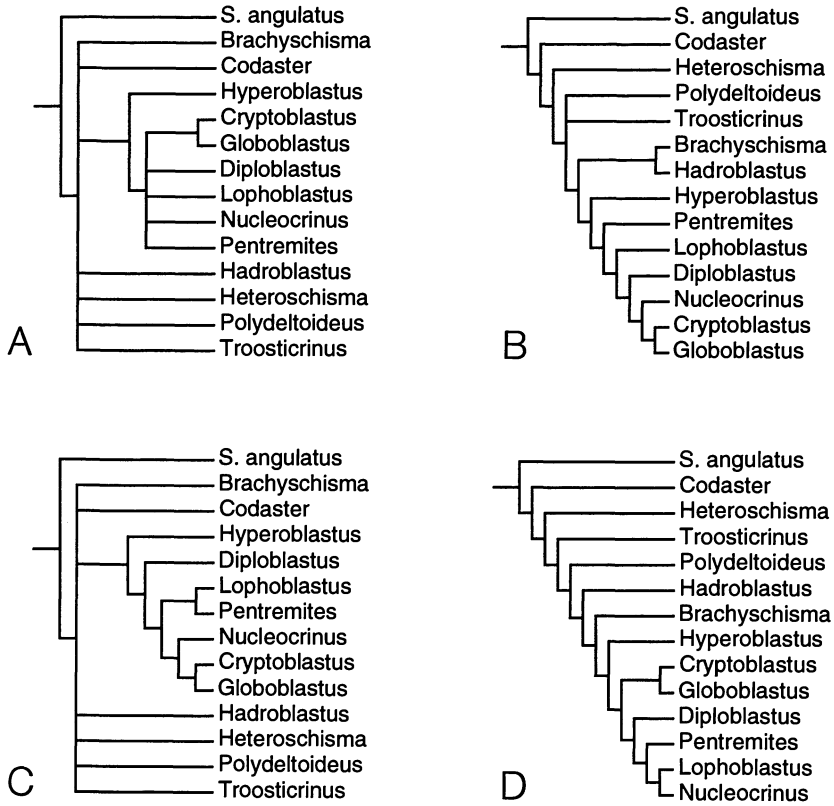

FIG. 8—Exact cladistic analyses of 13 blastoid species, drawn from 12 different families, and 1 outgroup. A, Consensus of 38 cladograms derived from analysis of standard characters excluding crystallographic data. B, Consensus of 2 cladograms from alternative coding of transitions among configurations of anal deltoid plates. C, Consensus of 6 cladograms from *a priori* division of quantitative characters rather than gap coding. D, Single cladogram from analysis employing selective character weighting rather than equal weighting.

65 and 66) yields a more modest restructuring of the consensus results (Fig. 12). Much of the cladogram is identical to the standard cladogram (Fig. 9), as might be expected since many transitions between states are the same in either coding scheme. Where the cost of transitions between anal deltoid arrangements varies, however, even by a single step, some taxa are affected. In particular, the transition between anal deltoid configurations in *Polydeltoideus*, which has paradeltoids, and *Pentremitidea*, which has cryptodeltoids, entails two evolutionary steps under the standard coding but three in the alternative coding. Under the alternative coding, *Polydeltoideus* moves from being the sister-taxon of *Pentremitidea* to being the sister of *Decaschisma* and *Leptoschisma*, which both have subdeltoids and are a single evolutionary step from the *Polydeltoideus* condition under either hypothesis. The different results obtained under the two anal deltoid coding schemes suggest that the blastoid data matrix is relatively sensitive to even small coding changes.

In contrast, alternative codings for the posterior hydrospire folds (characters 15 and 16 versus 96 and 97) produce negligible changes, inducing uncertainty in the placement of *Dentiblastus* as the sister to either *Anthoblastus* or *Astrocrinus* but producing no other differences from the standard cladogram. This suggests that the two different codings for posterior hydrospire folds carry nearly equivalent information.

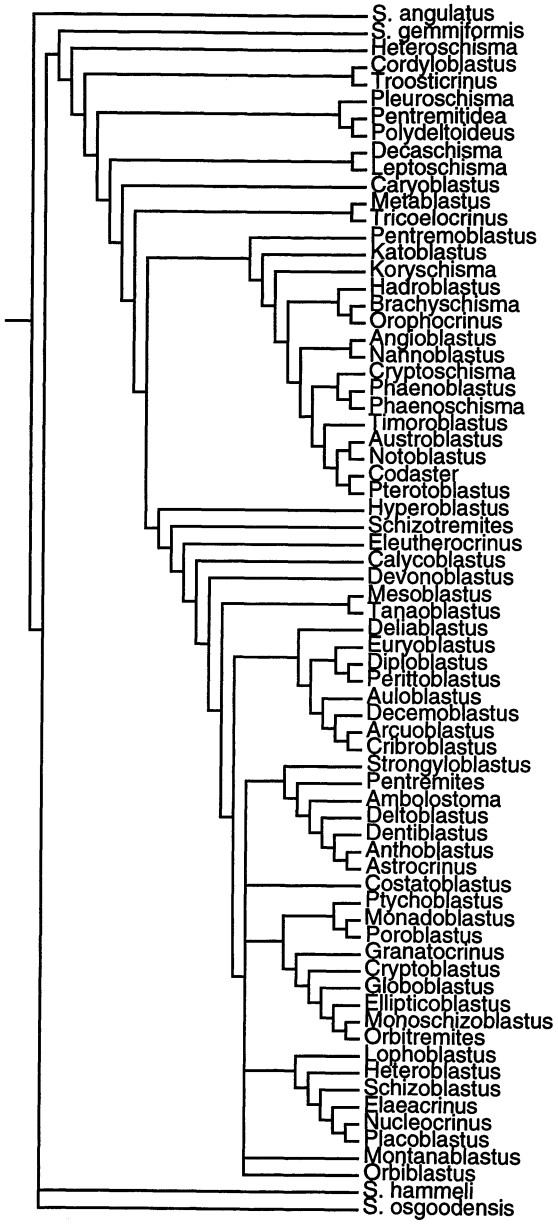

FIG. 9—Standard characters, without crystallography, under selective weighting. Strict consensus of 6 cladograms found when the standard characters of the 71 taxa in Table 2, less crystallographic characters 92-94, are weighted as in Table 4. This standard cladogram can be compared with cladograms resulting from alternative coding decisions. Cladograms summarized by the consensus have length = 6007, CI = 0.228, RI = 0.587, and RC = 0.134.

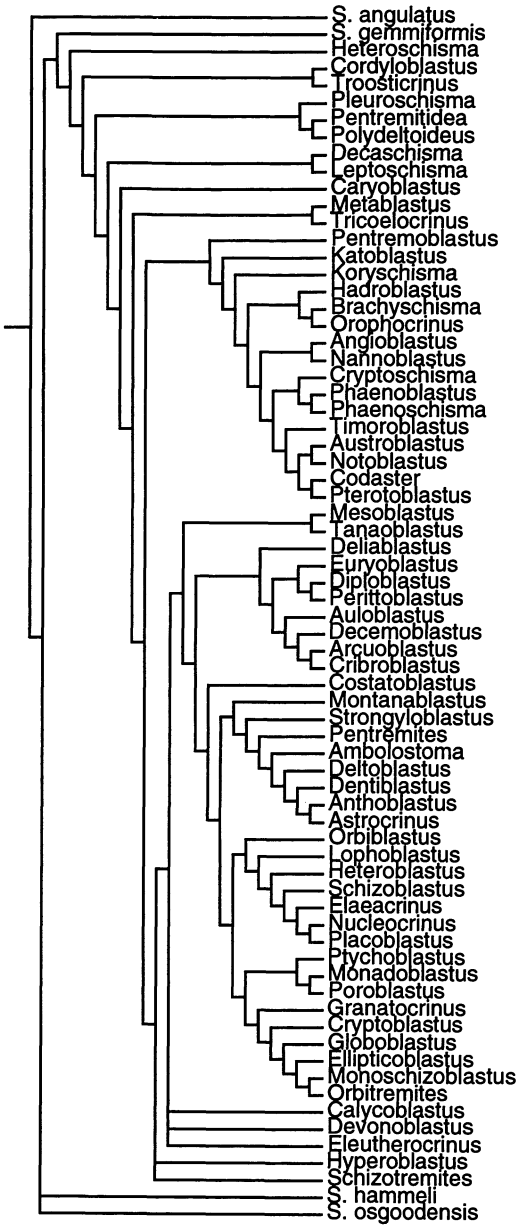

FIG. 10—Alternative determination of states in continuously-varying data. Strict consensus of 4 cladograms, summarizing relationships among 71 taxa according to selectively-weighted heuristic analysis of standard character codings, but with crystallographic characters 92-94 excluded and gap-coded characters 87-91 replaced by characters 98-101, which were arbitrarily subdivided into states before analysis. Cladograms summarized by the consensus have length = 6000, CI = 0.226, RI = 0.581, and RC = 0.131.

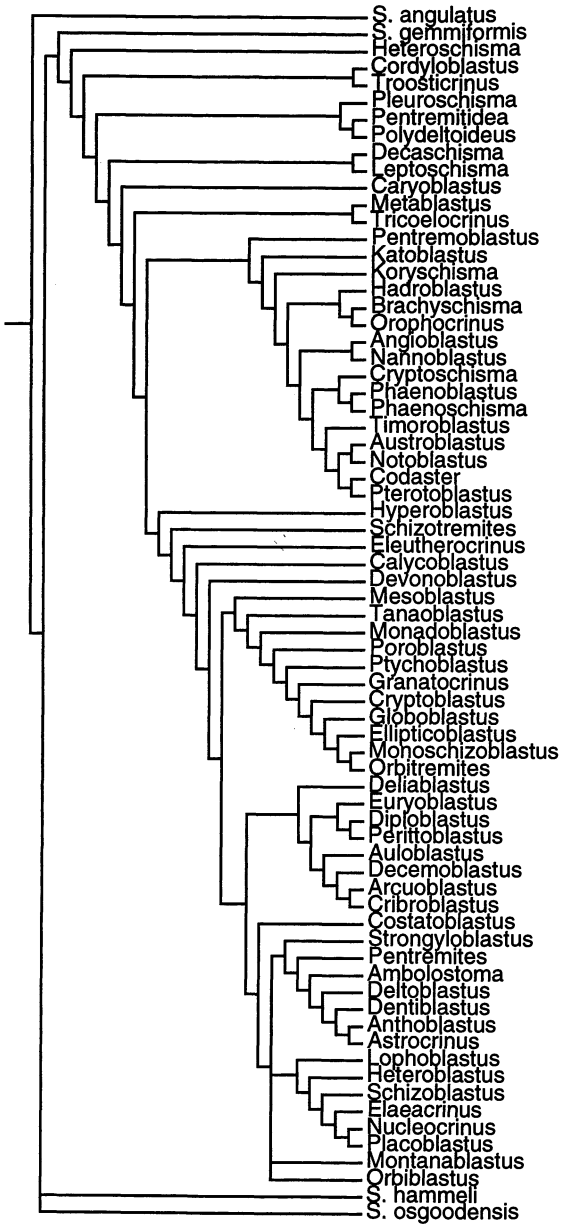

FIG. 11—Inclusion of crystallographic data. Strict consensus of 9 cladograms, summarizing relationships among 71 taxa according to selectively-weighted heuristic analysis of standard character codings, including characters 92-94. Cladograms summarized here have length = 6220, CI = 0.226, RI = 0.586, and RC = 0.132.

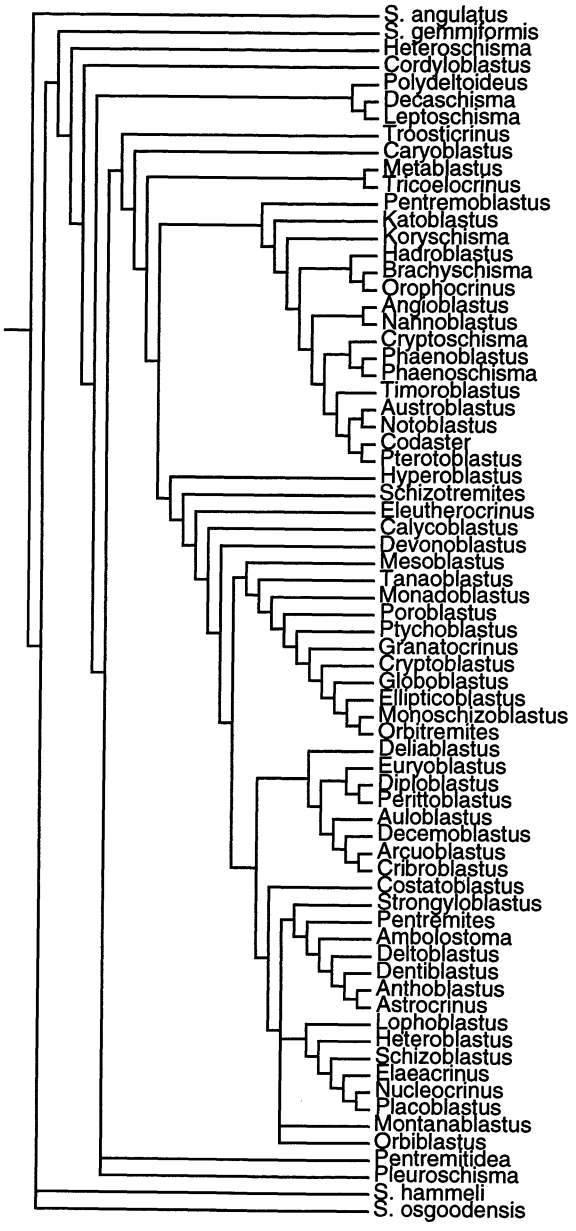

FIG. 12—Alternative coding of anal deltoids. Strict consensus of 18 cladograms, summarizing relationships among 71 taxa according to selectively-weighted heuristic analysis of standard character codings, but with crystallographic characters 92-94 excluded and characters 102-106 substituted for 65 and 66. Cladograms summarized by the consensus have length = 6057, CI = 0.226, RI = 0.584, and RC = 0.132.

FIG. 13—Selective character weighting, without crystallography. Strict consensus of 30 cladograms, summarizing relationships among 68 taxa according to heuristic analysis of standard character codings, but with crystallographic characters 92-94 excluded. Consensus summarizes cladograms having length = 5902, CI = 0.229, RI = 0.577, and RC = 0.132.

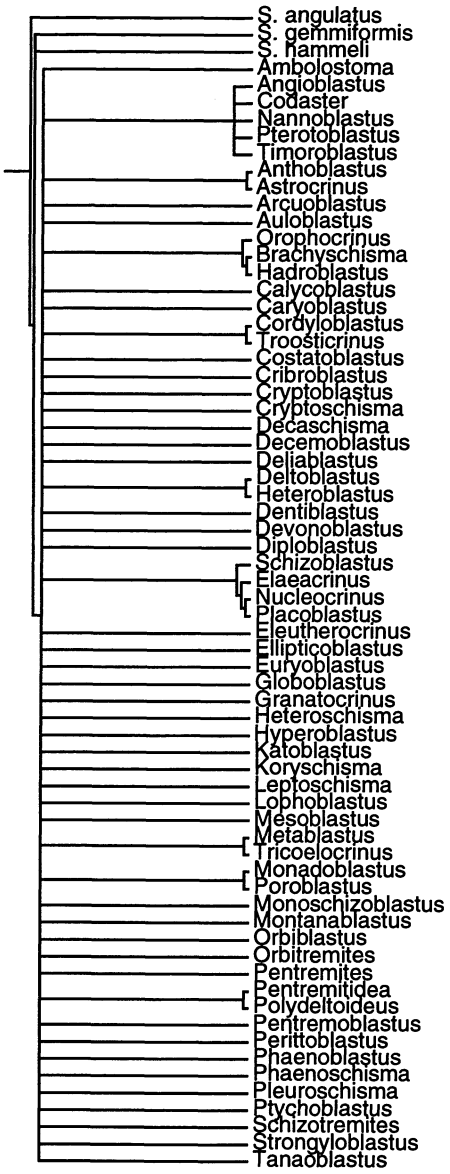

FIG. 14—Equal character weighting, without crystallography. Strict consensus of 6956 cladograms, summarizing relationships among 68 taxa according to heuristic analysis of standard character codings, but excluding crystallographic characters 92-94. Consensus summarizes cladograms having length = 652, CI = 0.222, RI = 0.596, and RC = 0.133.

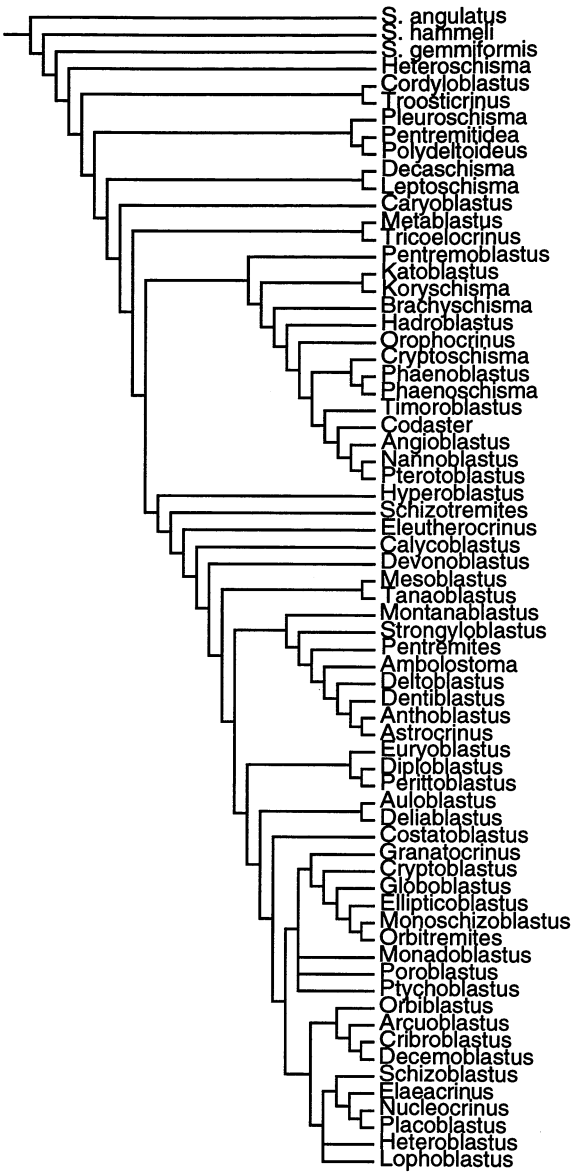

FIG. 15—Selective character weighting, with crystallography. Strict consensus of 10 cladograms, summarizing relationships among 68 taxa according to heuristic analysis of standard character codings, including crystallographic characters 92-94. Consensus summarizes cladograms having length = 6106, CI = 0.227, RI = 0.576, and RC = 0.131.

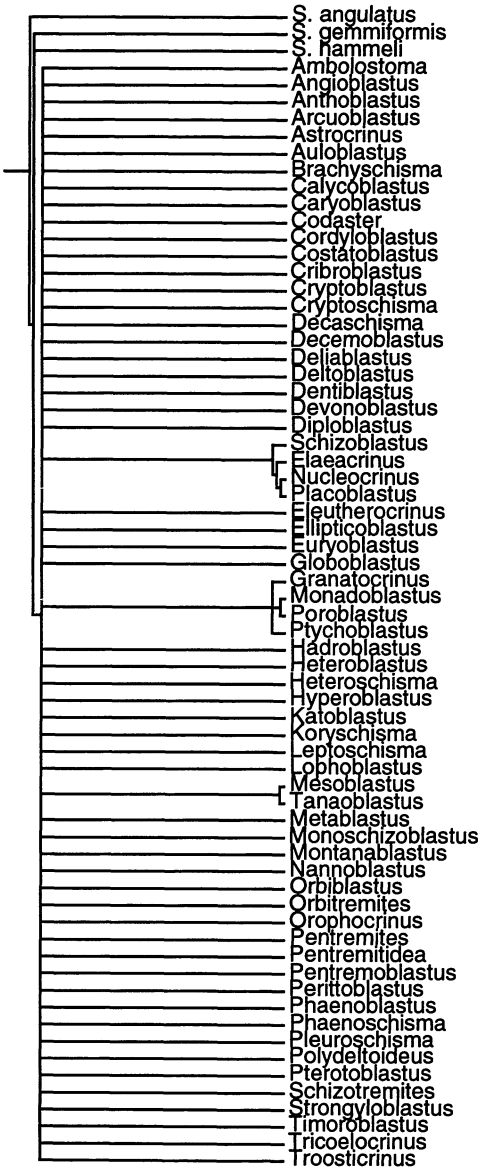

FIG. 16—Equal character weighting, with crystallography. Strict consensus of 14498 cladograms depicting relationships among 68 taxa according to heuristic analysis of standard character codings, including crystallographic characters 92-94. Consensus summarizes cladograms having length = 687, CI = 0.221, RI = 0.597, and RC = 0.132.

The importance of the differences between cladograms lies beyond the particulars of the different topologies or unstable taxa. The comparisons of alternative character codings in fact illustrate three general items worthy of note. The first is that, while not all changes in character coding are guaranteed to affect the resulting hypothesis (e.g., the coding of posterior hydrospire folds), individual coding changes have the potential to produce significant changes in cladogram topology (as with the coding of anal deltoid plates). The blastoid data matrix therefore does not strongly support a single preferred set of relationships but instead is rather sensitive to coding decisions in individual characters. A second, fully expected result is that the coding schemes that introduce the largest changes relative to the standard cladogram (Fig. 9) are those with characters that carry full weight under the selective weighting scheme (Table 4). Characters that are deweighted because of their arbitrary subdivision into states have lesser effects on the results. The third point, that the number of characters that vary in alternative codings influences the results, is related to the second since cumulative changes in character coding can be viewed as a form of weighting. Changing several deweighted characters may have equal or greater impact than changing a single fully-weighted one. In summary, choices regarding the coding of particular features can definitely affect the placement of individual taxa, as with *Polydeltoideus* (Fig. 12), especially when the coding scheme involves multiple characters. The influence of a particular character coding on overall cladogram topology, however, is subordinate to the more general choice of a protocol for weighting the data set as a whole.

As in the limited analysis of 14 taxa, stratigraphic data can again serve as an independent yardstick for measuring the relative success of the various coding methods. Unlike the results from the 14-taxon data set, however, evaluation of the full complement of 71 taxa by stratigraphic congruence does not suggest a great difference between coding schemes. All cladograms from the standard character coding (Fig. 9) had stratigraphic parsimony debts of 155, as did the most stratigraphically compatible cladograms from the analyses that examined crystallographic data and the alternative coding of posterior hydrospire folds. The alternative coding of anal deltoid transitions (Fig. 12) yielded results that are more compatible with stratigraphic order than are the standard coding results, but only by 1 unit of stratigraphic parsimony debt. As in the previous analysis, *a priori* division of characters into states (Fig. 10) produced results less compatible with stratigraphy than did the gap coding of the standard analysis, the best *a priori* coded cladograms having a stratigraphic parsimony debt of 158. All in all, compatibility with stratigraphy does not strongly favor one coding scheme for the full data set over all others, although unlike results from the limited analysis, some alternatives to the standard coding are equally or slightly more compatible with the stratigraphic order of fossil occurrences.

The cladograms from all comparative analyses share a great deal of common structure, which may account for the relatively small amount of variation in compatibility with stratigraphy shown by the alternative analyses of the full data set. Results from the limited set of taxa suggest that the selective weighting protocol provides the structure seen in the full analysis.

The cumulative influence of differential weighting can be examined further by comparing cladograms derived from equal and differential weighting of the full data set's standard coding. Preliminary analyses of equally-weighted data sets produced large numbers of equally-parsimonious cladograms. To reduce the number of cladograms and speed search times three incompletely coded taxa, the outgroup species *Stephanocrinus osgoodensis* and the two neoschismatids *Austroblastus whitehousei* and *Notoblastus stellaris*, were dropped from the analysis. In addition to facilitating comparisons of weighting conventions, the exclusion of these taxa incidentally demonstrates the influence that the number of taxa can have on the analysis. Removal of the three taxa and reanalysis of the standard character set (without crystallographic characters) under selective weighting actually increases the number of equally-parsimonious cladograms from 6 to 30 (Fig. 13) and yields a consensus substantially different

from that produced by all 71 taxa (Fig. 9). While both analyses yield similar general groupings of taxa, the cladograms with 68 taxa differ from those with 71 taxa in the detailed arrangements of taxa within larger clades. This is true both in the distal fissiculate clade (*Pentremoblastus* through *Nannoblastus*) from which *Austroblastus* and *Notoblastus* were removed, and among the spiraculates (e.g., *Auloblastus* and the position of the *Granatocrinus* clade), which retain the same taxa in both analyses. Thus, the blastoid data matrix is relatively sensitive to the addition and deletion of taxa as well as to the alteration of individual character codings.

Weighting and crystallography.—Returning to the question of the cumulative influence of equal versus selective character weighting, an equal-weighting analysis of the standard character codings (less crystallographic characters) for 68 taxa yields at least 6956 equally-parsimonious cladograms. The consensus from these (Fig. 14) can be compared with the selectively-weighted cladograms of Figure 13, but the equal weighting consensus is so much less resolved that comparison is almost moot. An observation of minor interest is that one of the few resolved relationships under equal weighting, uniting *Monadoblastus* and *Poroblastus*, is unresolved under the selective-weighting protocol. In contrast with results from the comparison of weights in the small data set, the selectively weighted analysis not only produces greater resolution but also is slightly more compatible with the stratigraphic ordering of fossils than are results from the equally-weighted analysis. Some cladograms with selective weighting have 136 units of stratigraphic parsimony debt, compared with 137 units for the most compatible cladograms from the equal-weighting analysis.

Adding crystallographic characters to the equally- and selectively-weighted analyses induces minor changes in cladogram topology. Addition of crystallographic data to the selective-weighting analysis of 68 taxa yields slightly more resolution in the positioning of small spiraculate subclades and reshuffles relationships among *Angioblastus*, *Nannoblastus*, and *Pterotoblastus* (Fig. 15, compare with Fig. 13). In the equal-weighting analysis of 68 taxa, addition of crystallographic characters further reduces the resolution of the strict consensus, yielding 14498 known equally-parsimonious cladograms (Fig. 16). Again, comparison with the stratigraphic record shows that cladograms from the selective-weighting analysis, with as few as 137 units of stratigraphic parsimony debt, are more compatible with the stratigraphic record that those from equal weighting, with a minimum of 141 units of stratigraphic parsimony debt.

DISCUSSION

Preferred character codings.—Cladistic analysis relies on character recognition and coding, and the choice of a final cladogram should be based on consideration of the characters rather than examination of cladogram topologies. Character evaluation can be done *a posteriori*, by comparing cladograms with data that were not involved in the initial analysis. Stratigraphic data serve as a basis for *a posteriori* character evaluation in this analysis, but on the whole show fairly similar levels of congruence among the different coding and weighting comparisons. If independent data are equivocal or unavailable, the choice of a cladogram should be based on an evaluation of characters and coding choices done before analyses are run and cladograms produced. After such an *a priori* evaluation alternative codings can be explored to determine the sensitivity of the results to coding decisions, but the cladograms from these analyses should not be viewed as competing with one another for selection as the preferred cladogram. The results presented here show clearly why this is the case. The matrix of blastoid morphological data does not point strongly to any one hypothesis of blastoid phylogeny and is sensitive to coding decisions affecting even single characters. Many cladograms are thus possible with just minor adjustments of the data. To choose a cladogram, and the coding that produced it, based on an inspection and comparison of cladogram topologies is to assume the results that were the goal of the phylogenetic analysis.

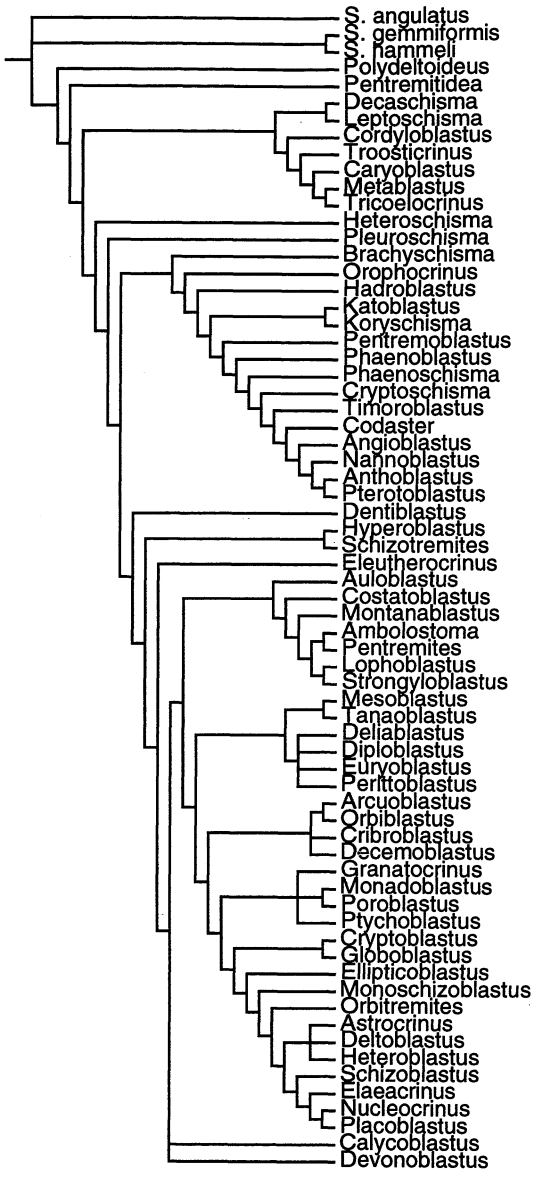

FIG. 17—Consensus of cladistic hypotheses under preferred coding of blastoid morphological characters. This is a strict consensus of the 96 cladograms from Figure 16 most compatible with stratigraphic ordering of taxa. See Figure 18 for arrangements of taxa that vary among the hypotheses.

Among the various coding options discussed in previous sections, the standard character codings marked in Table 2 were chosen *a priori* as the best available treatments and interpretations of blastoid morphology. As the comparisons with alternative codings have shown (Figs. 9-12), interpretations of morphology and hypotheses of transitions between morphological states are nontrivial, directly affecting the phylogenetic results. As an acknowledgment of the dependence of the preferred hypothesis of blastoid relationships on the

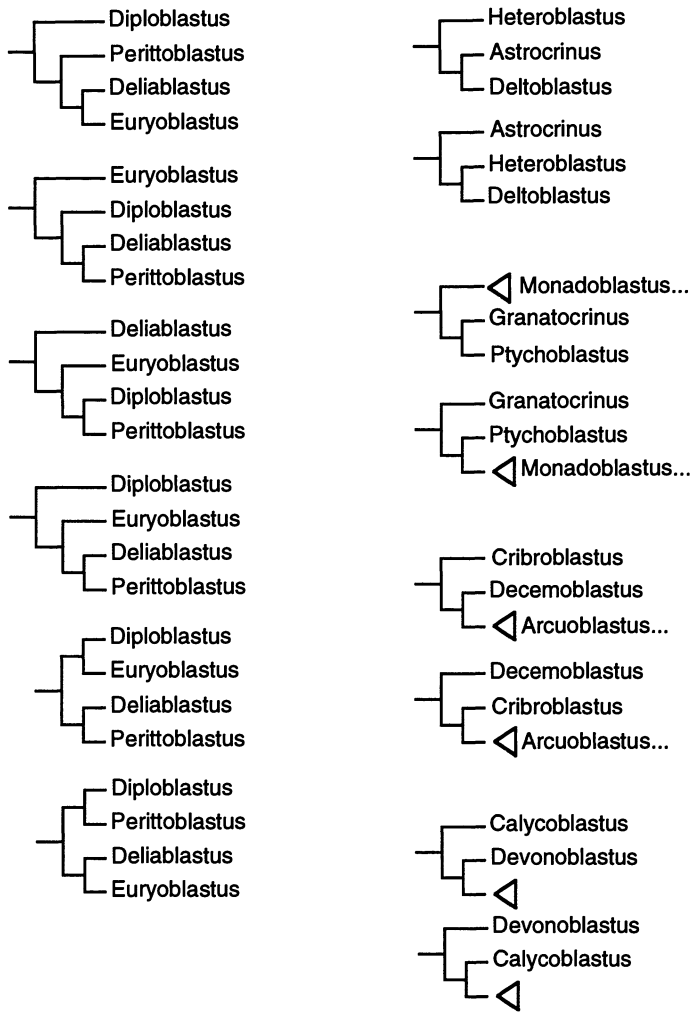

FIG. 18—Equally-parsimonious arrangements of taxa under preferred coding of blastoid morphological characters. Cladograms here show alternative positions of taxa that vary among the 96 cladograms summarized by the consensus cladogram of Figure 17. Triangles represent invariant distal clades. Ellipsis after a name indicates the taxon is one member of a larger clade.

initial assumptions, an attempt has been made to set forth the assumptions implicitly in the data matrix and explicitly in the text and appendix.

Among the standard character codings, the preferred data include crystallographic characters. The separate treatment of crystallography in comparative analyses is not because crystallographic characters differ in kind from other quantitative morphological characters. Rather, crystallography has been treated separately to examine its influence as a new source of character data. As applied to phylogenetics, crystallography can be a noisy source of phylogenetic information, with the three crystallographic characters' consistency indices ranging from 0.15 to 0.21 on a representative of the selectively-weighted cladograms (Fig. 15) and from 0.18 to 0.25 on a representative of the equally-weighted cladograms (Fig. 16). Despite the homoplasy shown by these characters, the tenet of total evidence holds that they should not

be dismissed, but should contribute what information they can to the analysis (Kluge, 1989; Eernisse and Kluge, 1993). The other characters will have to hold their own against any intrinsic homoplasies, with character congruence in the data set as a whole acting as the final arbiter of which characters are interpreted as homoplasious and which as phylogenetically informative.

Equal weighting has been chosen as the preferred weighting protocol because it is consistent with the assumption, made in recognizing and coding character states, that states are independent evolutionary derivations. While arbitrarily-divided characters may artificially subdivide evolutionary states, providing some justification for selective rather than equal weighting of characters, binary characters may likewise lump diverse states and the analysis should not necessarily accord them an advantage over selectively-deweighted multistate characters for doing so. An *a priori* evaluation of coding therefore favors the results of an analysis of the standard character codings, plus crystallographic characters, with equal weighting.

Unfortunately, the blastoid data matrix provides no unique solution for the preferred coding (Fig. 16), yielding instead at least 14498 equally-parsimonious cladograms. Whether more equally-parsimonious cladograms exist is unknown. Morphological data under the favored coding therefore yield a highly unspecified hypothesis that is sensitive to small changes in character coding.

Cladograms congruent with stratigraphy.—Although character evidence is unable to sort among the competing cladistic hypotheses, independent data on the stratigraphic order of appearance of fossils can be useful in evaluating the competing cladograms (Suter, 1993, 1994). Of the 14498 equally-parsimonious cladograms found in heuristic searches of the preferred characters, 96 emerge as equally most compatible with blastoid stratigraphic order. Figure 17 presents a consensus of these 96 cladograms, which vary in the relative placements of five different sets of taxa (Fig. 18). The consensus cladogram of Figure 17 is the best-supported summary hypothesis of blastoid relationships as elucidated from morphological evidence and evaluated by compatibility with the stratigraphic record.

The cladogram derived from parsimony-based cladistic analysis of morphological data (Fig. 17) differs substantially from previous hypotheses of blastoid relationships (Fay, 1967; Breimer and Macurda, 1972; Horowitz et al., 1986; Waters and Horowitz, 1993). Detailed comparisons of character evolution, the correspondence of phylogeny with taxonomy, or particular relationships among species are unwarranted at this point, however, because inclusion of stratigraphic data in the construction of hypotheses in a stratocladistic analysis will yield a phylogenetic tree that is globally more parsimonious than the best morphological cladograms (Bodenbender and Fisher, ms.).

The multitude of cladograms found when all evolutionary changes are given equal weight (Fig. 16) suggests that there is little congruence among all characters, as confirmed by the ensemble consistency index (CI) of 0.221 and ensemble retention index (RI) of 0.597, which yield an ensemble rescaled consistency index (RC) of 0.132. (Indices are calculated for fully-resolved representatives drawn from the equally-parsimonious cladograms. In the interest of consistent comparisons between analyses, tree lengths and indices are calculated for all characters participating in each analysis, regardless of whether or not some are uninformative under particular coding assumptions. Exclusion of uninformative characters changes tree lengths and indices trivially, rarely by more than 1%.) Investigation of the equally-parsimonious cladograms shows that several taxa and clades are highly variable in position on the cladogram, and that the lack of resolution is not solely attributable to the jumping of incompletely coded taxa from place to place on the cladogram, a common source of poor resolution in cladistic analyses. The lack of any pattern coming to the fore under equal character weighting may reflect natural morphological variability in blastoids, or it may in part result from arbitrarily-recognized character states conflicting with one another. The better resolution of the selectively weighted analyses (Figs. 13 and 15) may result from dampening

of noise in the arbitrarily-divided characters, which is the justification for selecting a selective weighting protocol. More likely, however, the resolution with selective weighting is not attributable to a filtering of noise but to the aggregate structuring effect of the most strongly weighted characters, which may themselves still be phylogenetically noisy. Tree statistics for the selectively weighted analysis with crystallographic data included (Fig. 15; CI = 0.227, RI = 0.576, RC = 0.131) support this latter interpretation since they are calculated with individual character weights taken into account but are very similar to the values of the equally-weighted analysis (Fig. 17). Apparently the incomplete coding of quantitative and crystallographic characters is not a major factor in the lack of resolution. Of the 68 taxa, only 53 have three or more of the five quantitative characters coded and only 47 are coded for at least one crystallographic character. Although the two sets of characters each yield different consensus cladograms when included in analyses (compare Fig. 9 with Figs. 10 and 11), they do not necessarily yield large numbers of minimum length cladograms.

SUMMARY

Cladistic analysis of morphological data yields a hypothesis of blastoid relationships that differs from previous hypotheses both in the specific placement of individual taxa and in relationships among larger clades. As with most cladistic analyses, the analysis of blastoid morphological data is sensitive to the inclusion or exclusion of taxa, the weighting of characters, and individual decisions on how to encode complex morphological features. Because of this sensitivity, character coding schemes should be evaluated and the best-supported coding protocol designated before analyses are run.

Congruence with independent data in the form of order of occurrence of fossils in the stratigraphic record is an additional means of evaluating character codings, and may be applied after analyses are run. In the blastoid data, congruence with stratigraphy does not strongly favor some character coding schemes relative to others, leaving *a priori* determination of preferred codings as the favored means of choosing a coding protocol. Congruence with stratigraphy does, however, provide a very effective means of evaluating alternative cladograms that are equally parsimonious according to morphological data alone. Out of 14498 equally-parsimonious cladograms of blastoid generic relationships, 96 could be designated as most congruent with the stratigraphic record.

Crystallographic data in the form of orientations of crystallographic axes are moderately homoplasious as evaluated by character congruence. Retention indices for the three crystallographic characters (r ranging from 0.50 to 0.73, rc from 0.11 to 0.18) are on a par with the ensemble RI and RC values for the data set as a whole, and suggest that crystallographic data have neither a greater nor a lesser claim to phylogenetic insight than any other quantitative morphological data. Although not exceptionally robust, crystallographic information is a source of morphological data that has rarely been tapped in phylogenetic analyses of echinoderms but can appreciably influence the final interpretation of phylogeny.

ACKNOWLEDGMENTS

I thank A. S. Horowitz for sharing ideas on blastoid character coding, and M. Foote for generously making available quantitative data on blastoid morphology. This work also benefited from discussions with H. H. Beaver, R. K. Carr, W. C. Clyde, B. Dyer, D. J. Eernisse, D. B. Macurda, Jr., R. F. Stearley, M. D. Uhen, and J. A. Waters. I am grateful to J. W. M. Thompson (USNM), F. J. Collier (MCZ), M. Topor (Hamtramck, Michigan) and particularly A. Fabian (Temperance, Michigan) for permission to examine and prepare specimens, and the Museum of Zoology Fish Division, Exhibit Museum, Clements Library,

and Information Technology Division of the University of Michigan for access to computing resources. D. C. Fisher, T. M. Collins, M. Foote, P. D. Gingerich, and G. R. Smith provided advice and assistance throughout this project as well as insightful comments on earlier drafts of the manuscript. B. J. Miljour assisted with illustrations. I also wish to acknowledge the support of a Paleontological Society/Margaret C. Wray Trust grant-in-assistance, a Geological Society of America Research Grant, the Scott Turner Fund of the University of Michigan Department of Geological Sciences, and National Science Foundation grant SBR-9211984 to D. C. Fisher.

LITERATURE CITED

AAPG. 1985a. COSUNA—Midwestern Basin and Arches Region correlation chart. R. H. Shaver, coordinator.

———. 1985b. COSUNA—Northern Appalachian Region correlation chart. D. G. Patchen, K. L. Avary, and R. B. Erwin, coordinators.

———. 1987. COSUNA—Mid-Continent Region correlation chart. F. J. Adler, coordinator.

AUSICH, W. I. and D. L. MEYER. 1988. Blastoids from the late Osagean Fort Payne Formation (Kentucky and Tennessee). Journal of Paleontology, 62: 269-283.

BEAVER, H. H. 1961a. Morphology of the blastoid *Globoblastus norwoodi*. Journal of Paleontology, 35: 1103-1112.

———. 1961b. *Auloblastus*, a new blastoid from the Mississippian Burlington Limestone. Journal of Paleontology, 35: 1113-1116.

———, R. O. FAY, D. B. MACURDA, JR., R. C. MOORE, and J. WANNER. 1967. Blastoids. In R. C. Moore (ed.), Treatise on Invertebrate Paleontology. Part S. Echinodermata 1. Geological Society of America and the University of Kansas, Boulder, Colorado, and Lawrence, Kansas, pp. S298-S455.

———, ———, and R. C. MOORE. 1967. Anal deltoids. In R. C. Moore (ed.), Treatise on Invertebrate Paleontology. Part S. Echinodermata 1. Geological Society of America and the University of Kansas, Boulder, Colorado, and Lawrence, Kansas, pp. S315-S323.

BODENBENDER, B. E. 1990. Crystallography of Edrioasteroid Ambulacral Cover Plates. Unpublished Master's thesis, University of Michigan, Ann Arbor, 24 pp.

———. 1993. Crystallographic patterns in blastoid skeletal elements. Geological Society of America, Abstracts with Programs, 25(6): A55.

———. 1994. Skeletal Crystallography in Cladistic and Stratocladistic Investigations of Blastoid Phylogeny. Unpublished Ph.D. dissertation, University of Michigan, Ann Arbor, 287 pp.

———. 1996. Patterns of crystallographic axis orientation in blastoid skeletal elements. Journal of Paleontology, in press.

BREIMER, A. 1988a. The anatomy of the spiraculate blastoids. Part I: The family Troosticrinidae. Proceedings of the Koninklijke Nederlandse Akademie van Wetenschappen, Series B, 91: 1-13.

———. 1988b. The anatomy of the spiraculate blastoids. Part II: The family Diploblastidae. Proceedings of the Koninklijke Nederlandse Akademie van Wetenschappen, Series B, 91: 161-169.

——— and A. J. DOP. 1975. An anatomic and taxonomic study of some Lower and Middle Devonian blastoids from Europe and North America. I and II. Proceedings of the Koninklijke Nederlandse Akademie van Wetenschappen, Series B, 78: 39-61.

——— and K. A. JOYSEY. 1968. Anatomical studies of *Orbitremites* and *Ellipticoblastus* (Blastoidea). I and II. Proceedings of the Koninklijke Nederlandse Akademie van Wetenschappen, Series B, 71: 175-202.

——— and D. B. MACURDA. 1965. On the systematic position of some blastoid genera from the Permian of Timor. Proceedings of the Koninklijke Nederlandse Akademie van Wetenschappen, Series B, 68: 209-217.

——— and ———. 1972. The phylogeny of the fissiculate blastoids. Verhandelingen der Koninklijke Nederlandse Akademie van Wetenschappen, Afdeling Natuurkunde, Eerste Reeks, 26(3): 1-390.

———, ———, and R. J. PROKOP. 1968. New Lower Devonian blastoids from Bohemia. Proceedings of the Koninklijke Nederlandse Akademie van Wetenschappen, Series B, 71: 124-136.

——— and H. A. VAN EGMOND. 1968. A new development of the acetate peel technique for use on fossil echinoderms. Proceedings of the Koninklijke Nederlandse Akademie van Wetenschappen, Series B, 71: 144-149.

BRETT, C. E., T. J. FREST, J. SPRINKLE, and C. R. CLEMENT. 1983. Coronoidea: a new class of blastozoan echinoderms based on taxonomic reevaluation of *Stephanocrinus*. Journal of Paleontology, 57: 627-651.

BROADHEAD, T. W. 1984. *Macurdablastus*, a Middle Ordovician blastoid from the southern Appalachians. University of Kansas Paleontological Contributions, Paper 110: 1-9.

CHILDS, O. E. 1985. Correlation of stratigraphic units of North America—COSUNA. American Association of Petroleum Geologists Bulletin, 69: 173-180.

CLINE, L. M. 1936. Blastoids of the Osage group, Mississippian: Part I. The genus *Schizoblastus*. Journal of Paleontology, 10: 260-281.

CONRAD, T. A. 1842. Observations on the Silurian and Devonian systems in the United States, with descriptions of new organic remains. Journal of the Academy of Natural Sciences of Philadelphia, 8: 228-280.

DONOGHUE, M. J., J. A. DOYLE, J. GAUTHIER, A. G. KLUGE, and T. ROWE. 1989. The importance of fossils in phylogeny reconstruction. Annual Reviews of Ecology and Systematics, 20: 431-460.

DONOVAN, S. K. and C. R. C. PAUL. 1985. Coronate echinoderms from the Lower Paleozoic of Britain. Palaeontology, 28: 527-543.

EERNISSE, D. J. and A. G. KLUGE. 1993. Taxonomic congruence versus total evidence, and amniote phylogeny inferred from fossils, molecules, and morphology. Molecular Biology and Evolution, 10: 1170-1195.

ETHERIDGE, R., JR. and P. H. CARPENTER. 1886. Catalogue of the Blastoidea in the Geological Department of the British Museum (Natural History). British Museum (Natural History), London, 322 pp.

FARRIS, J. S. 1988. Hennig86. Version 1.5. Computer program distributed by its author, Port Jefferson Station, New York.

FAY, R. O. 1960. *Ptychoblastus*, a new Mississippian blastoid from Missouri. Journal of Paleontology, 34: 1198-1201.

———. 1961a. The type of *Monoschizoblastus* Cline, 1936. Oklahoma Geology Notes, 21: 173-175.

———. 1961b. Blastoid studies. The University of Kansas Paleontological Contributions, Echinodermata, Article 3, 147 pp.

———. 1961c. Type of *Schizotremites*, a Devonian blastoid from New York. Oklahoma Geology Notes, 21: 331-333.

———. 1962. *Strongyloblastus*, a new Devonian blastoid from New York. Oklahoma Geology Notes, 22: 132-135.

———. 1967. Phylogeny and evolution. In R. C. Moore (ed.), Treatise on Invertebrate Paleontology. Part S. Echinodermata 1. Geological Society of America and the University of Kansas, Boulder, Colorado, and Lawrence, Kansas, pp. S392-S396.

——— and J. W. KOENIG. 1963. *Pentremoblastus*, a new Lower Mississippian blastoid from Illinois. Oklahoma Geology Notes, 23: 267-270.

FISHER, D. C. 1982. Phylogenetic and macroevolutionary patterns within the Xiphosurida. Third North American Paleontological Convention, Proceedings, 1: 175-180.

———. 1988. Stratocladistics: integrating stratigraphic and morphologic data in phylogenetic inference. Geological Society of America, Abstracts with Programs, 20(7): A186.

———. 1991. Phylogenetic analysis and its application in evolutionary biology. In N. L. Gilinsky and P. W. Signor (eds.), Analytical Paleobiology. Short Courses in Paleontology 4, Paleontological Society, pp. 103-122.

———. 1992. Stratigraphic parsimony. In W. P. Maddison and D. R. Maddison, MacClade: Analysis of Phylogeny and Character Evolution. Version 3.0. Sinauer Associates, Sunderland, Massachusetts, pp. 124-129.

———. 1994a. Measures of congruence between stratigraphic data and phylogenetic hypotheses. Geological Society of America, Abstracts with Programs, 26(7): A123.

———. 1994b. Stratocladistics: morphological and temporal patterns and their relation to phylogenetic process. In L. Grande and O. Rieppel (eds.), Interpreting the Hierarchy of Nature. Academic Press, Inc., San Diego, pp. 133-171.

——— and B. E. BODENBENDER. 1993. CalcAxes: a program for computation of calcite crystallographic axis orientations. Contributions from the Museum of Paleontology, University of Michigan, 28: 327-363.

——— and R. S. COX. 1987. Phylogenetic applications of echinoderm skeletal crystallography. Geological Society of America, Abstracts with Programs, 19(7): 663.

——— and ———. 1988. Application of skeletal crystallography to phylogenetic inference in fossil echinoderms. In R. D. Burke, P. V. Mladenov, P. Lambert, and R. L. Parsley (eds.), Echinoderm Biology: Proceedings of the Sixth International Echinoderm Conference. A. A. Balkema, Rotterdam, p. 797.

FOOTE, M. 1991. Morphological and taxonomic diversity in a clade's history: the blastoid record and stochastic simulations. Contributions from the Museum of Paleontology, University of Michigan, 28: 101-140.

HOROWITZ, A. S., D. B. MACURDA, JR., and J. A. WATERS. 1986. Polyphyly in the Pentremitidae (Blastoidea, Echinodermata). Geological Society of America Bulletin, 97: 156-161.

KLUGE, A. J. 1989. A concern for evidence and a phylogenetic hypothesis of relationships among *Epicrates* (Boidae, Serpentes). Systematic Zoology, 38: 7-25.

MACURDA, D. B. 1962. Observations on the blastoid genera *Cryptoblastus*, *Lophoblastus*, and *Schizoblastus*. Journal of Paleontology, 36: 1367-1377.

———. 1964a. *Dentiblastus* - a new blastoid genus from the Burlington Limestone (Mississippian). Journal of Paleontology, 38: 367-372.

———. 1964b. The Mississippian blastoid genera *Phaenoschisma*, *Phaenoblastus*, and *Conoschisma*. Journal of Paleontology, 38: 711-724.

———. 1965. *Orbiblastus*, a new Mississippian blastoid genus from Arkansas. Papers of the Michigan Academy of Science, Arts, and Letters, 50: 299-307.

———. 1966. The ontogeny of the Mississippian blastoid *Orophocrinus*. Journal of Paleontology, 40: 92-124.

———. 1967. The Lower Carboniferous (Tournaisian) blastoids of Belgium. Journal of Paleontology, 41: 455-486.

———. 1972. The type species of the Permian blastoid *Calycoblastus*. Journal of Paleontology, 46: 94-98.

———. 1975. The *Pentremites* (Blastoidea) of the Burlington Limestone (Mississippian). Journal of Paleontology, 49: 346-373.

———. 1977a. Two Carboniferous blastoids from Scotland. Palaeontology, 20: 225-236.

———. 1977b. *Arcuoblastus* and *Decemoblastus*, two new Mississippian blastoid genera from the Burlington Limestone, Iowa. Journal of Paleontology, 51: 1201-1214.

———. 1978. The Mississippian blastoid genus *Cribroblastus*. Journal of Paleontology, 52: 1288-1293.

———. 1979. The ontogeny and taxonomy of the Mississippian blastoid genus *Schizoblastus*. Contributions from the Museum of Paleontology, University of Michigan, 25: 45-87.

———. 1983. Systematics of the fissiculate Blastoidea. Papers on Paleontology, the Museum of Paleontology, University of Michigan, no. 22: 1-291.

——— and A. BREIMER. 1977. *Strongyloblastus*, a Mississippian blastoid from western Canada. Journal of Paleontology, 51: 693-700.

MILLENDORF, S. A. 1979. The functional morphology and life habits of the Devonian blastoid *Eleutherocrinus cassedayi* Shumard and Yandell. Journal of Paleontology, 53: 553-561.

OLSON, E. C. and R. L. MILLER. 1958. Morphological integration. University of Chicago Press, Chicago, 317 pp.

PAUL, C. R. C. and A. B. SMITH. 1984. The early radiation and phylogeny of echinoderms. Biological Reviews, 59: 443-481.

PECK, R. E. 1930. Blastoids from Brazer limestones of Utah. Pan American Geologist, 54: 104-108.

RAUP, D. M. 1962a. The phylogeny of calcite crystallography in echinoids. Journal of Paleontology, 36: 793-810.

———. 1962b. Crystallographic data in echinoderm classification. Systematic Zoology, 11: 97-108.

SPRINKLE, J. 1973. Morphology and evolution of blastozoan echinoderms. Special Publication. Museum of Comparative Zoology, Harvard University, Cambridge, Massachusetts, 283 pp.

———. 1980. Origin of blastoids: new look at an old problem. Geological Society of America, Abstracts with Programs, 12(7): 528.

——— and R. C. GUTSCHICK. 1967. *Costatoblastus*, a channel fill blastoid from the Sappington Formation of Montana. Journal of Paleontology, 41: 385-402.

——— and ———. 1990. Early Mississippian blastoids from western Montana. Bulletin of the Museum of Comparative Zoology, Harvard University, 152: 89-166.

SUTER, S. J. 1993. Stratigraphic ranges as a basis for choosing among equally parsimonious phylogenies: the case of cassiduloid echinoids. Geological Society of America, Abstracts with Programs, 25(6): A105.

———. 1994. Cladistic analysis of cassiduloid echinoids: trying to see the phylogeny for the trees. Biological Journal of the Linnean Society, 53: 31-72.

SWIDERSKI, D. L., M. FOOTE, and B. E. BODENBENDER. 1993. Integrated shape change in elliptical globose blastoids. American Zoologist, 33(5): 71A.

SWOFFORD, D. L. 1993. PAUP: Phylogenetic Analysis Using Parsimony. Version 3.1. Computer program distributed by the Illinois Natural History Survey, Champaign, Illinois.

——— and D. P. BEGLE. 1993. PAUP: Phylogenetic Analysis Using Parsimony. Version 3.1. Users Manual. Smithsonian Institution, Washington, D. C., 257 pp.

WATERS, J. A. 1990. The palaeobiogeography of the Blastoidea (Echinodermata). In W. S. McKerrow and C. R. Scotese (eds.), Palaeozoic Palaeogeography and Biogeography. Geological Society Memoir, 12: 339-352.

——— and A. S. HOROWITZ. 1993. Ordinal-level evolution in the Blastoidea. Lethaia, 26: 207-213.

———, ———, and D. B. MACURDA, JR. 1985. Ontogeny and phylogeny of the Carboniferous blastoid *Pentremites*. Journal of Paleontology, 59: 701-712.

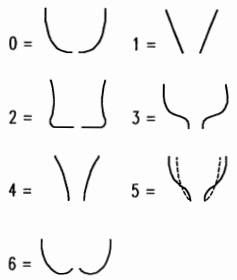

FIG. A1—Lateral profiles of lower portion of blastoid thecae, illustrating states of character 3. In 5, solid lines are profiles of rays; dashed lines are profiles of interrays.

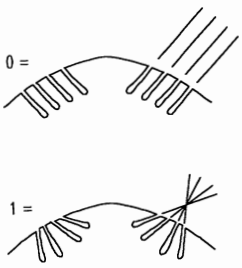

FIG. A2—Transverse section of hydrospire folds in a single blastoid interray, illustrating states of character 8. Exterior of theca is toward top of page. Lines indicate orientation of folds.

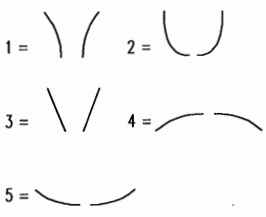

FIG. A3—Profiles of ambulacral sinus walls, looking adorally along ambulacrum, illustrating states of character 24. Exterior of specimen is toward top of page.

APPENDIX

CHARACTERS AND CHARACTER STATES

1. Widest portion of theca (looking at A ray in lateral view)
   - 0 = widest at adoral third
   - 1 = widest at middle third
2. Thecal width vs. height
   - 0 = width less than height
   - 1 = width greater than or equal to height
3. Lateral outline of pelvis (see Figure A1; 3.6 codes recessed basals)
   - 0 = convex
   - 1 = straight
   - 2 = sharply angled
   - 3 = laterally concave at base, broadly convex adorally
   - 4 = concave
   - 5 = convex interradially, recurved radially
   - 6 = aborally concave at base, broadly convex adorally
4. Summit plate configuration (condition of plates covering peristome)
   - 0 = 5-6 large, flat plates
   - 1 = many tiny plates in low pavement
   - 2 = plates elevated in pyramid
5. Hydrospire folds
   - 0 = absent
   - 1 = present
6. Total number of hydrospire folds per normal field (ordered; coding maximum number since number of folds may increase with ontogeny)
   - 1 = 1
   - 2 = 2
   - 3 = 3-4
   - 4 = 5-13
   - 5 = 33
7. Hydrospire folds on hypodeltoid
   - 0 = absent
   - 1 = present
8. Orientation of hydrospire folds in cross section (see Figure A2)
   - 0 = parallel
   - 1 = convergent
9. Hydrospire ducts (when variably developed, code most prevalent state)
   - 0 = no sharp differentiation of hydrospire fold into narrow and wide area
   - 1 = adaxial portion of hydrospire fold clearly and sharply expanded
10. Adoral opening for covered hydrospires (not applicable to specimens with completely exposed slits)
    - 0 = single opening
    - 1 = "paired spiracle" - opening partly divided by deltoid crest
    - 2 = double opening produced by narrow deltoid septum
    - 3 = double opening produced by wide deltoid tip
11. Hydrospire slit exposure (ordered; in part, codes presence of spiracular slit or spiracle; considered concealed if full slit is not visible lateral to ambulacrum; ends of slits emerging from beneath ambulacrum are not considered exposed)
    - 0 = concealed
    - 1 = some slits exposed laterally
    - 2 = exposed
12. Aboral ends of hydrospire slits emergent from beneath ambulacrum
    - 0 = not emergent
    - 1 = emergent

13. Placement of hydrospire slits (evaluate length of exposed and concealed slits in plan view; do not evaluate width of field)
    0 = slits open on deltoid and radial subequally
    1 = slits open mainly on radial
    2 = slits open mainly on deltoid
14. Length of open hydrospire cleft (Breimer and Macurda, 1972, usage; coded only for specimens with clefts, i.e., covered slits and no pores)
    0 = cleft less than half length of ambulacrum
    1 = cleft more than half length of ambulacrum
15. Anal area hydrospire folds (if the regular number of folds is present in at least one of the two posterior hydrospire fields, folds are counted as present in full number; coding does not distinguish whether folds are reduced in left or right field, as long as one field has full number of folds)
    0 = hydrospire folds absent in anal area
    1 = hydrospire folds present in anal area in full number
    2 = hydrospire folds present but reduced in number
16. Posterior hydrospire fold symmetry (contrasts asymmetry in number of hydrospire folds between the two sides of the posterior interray against symmetrical arrangement of folds, but implies an assumption that all symmetrical occurrences and absences of folds are homologous; while in general this may be an onerous assumption, for the current taxa character 16 is autapomorphic and therefore phylogenetically uninformative, so the assumed homology of symmetrical states does not come into play as information distinct from the absence and presence data coded in 15; alternative characters 96 and 97 code the number of folds in the two anal fields separately, so a change of state from folds absent to folds present in both fields is counted as 2 morphological changes under the alternative coding)
    0 = posterior hydrospire folds symmetrically distributed
    1 = hydrospire folds in C posterior field only
17. Anal opening confluent with adoral opening to hydrospire folds (17.2 corresponds to asymmetrical anispiracle; not applicable for specimens with widely exposed hydrospire slits)
    0 = confluent
    1 = not confluent
    2 = D-side opening confluent, C-side separate
18. Hydrospire pores penetrating radials and/or deltoids (first of two types of pores; pores between side plates do not necessarily indicate penetration of radials or deltoids)
    0 = absent
    1 = present
19. Hydrospire pores opening between side plates and radials and/or deltoids (second of two types of pores; includes pores opening at lateral margins of side plates)
    0 = absent
    1 = present
20. Pores surrounded by side plates (applies only to pores of character 19)
    0 = all pores bordered in part by radials and/or deltoids
    1 = pores are contained entirely within side and/or outer side plates at some point along ambulacrum
21. Ambulacral shape (coded for regular ambulacra of asymmetrical specimens, reduced ambulacra ignored)
    0 = parallel-sided
    1 = ovate, petaloid
    2 = rhombiform
    3 = lanceolate
22. Lateral view of ambulacra
    0 = ambulacra curved
    1 = ambulacra straight
23. Ambulacra confluent at oral end (side plates from different ambulacra touch or are connected by single intermediate side plate)
    0 = not confluent
    1 = confluent

24. Curvature of ambulacral sinus walls (see Figure A3; view sinus radially, looking along lancet, to get cross-section of radials and deltoids; ignore influence of ambulacrum on cross section)
    0 = sinus absent
    1 = walls convex toward center of ambulacrum
    2 = U-shaped; walls concave toward center of ambulacrum
    3 = walls straight
    4 = sinus inverted
    5 = broadly U-shaped
25. Ambulacra recessed or emergent
    0 = ambulacra recessed below edge of theca
    1 = ambulacra even with edge of theca
    2 = ambulacra emergent above level of theca
26. Abaxial surface of ambulacrum (see Figure A4; code general attitude of external surface of side plates as seen in end-on view of ambulacrum)
    0 = abaxial surface flat
    1 = abaxial surface concave
    2 = abaxial surface convex
27. Location of tips of ambulacra (ordered)
    0 = tips extend to top third of specimen
    1 = tips extend to middle third of specimen
    2 = tips extend to bottom third of specimen
    3 = tips extend to aboral edge of specimen
28. Invaginations alongside ambulacra (invaginations indent but do not penetrate plates bordering ambulacrum)
    0 = absent
    1 = present
29. Adorally-directed radial keel (keel is at aboral margin of ambulacral sinus, differs from character 72 by pointing adorally rather than laterally; formed by primaxil in *Stephanocrinus*)
    0 = absent
    1 = present
30. Ambulacral duct system within lancet (lobes on median groove at adoral end of lancet taken as evidence for lack of duct system)
    0 = absent
    1 = present
31. Maximum width of exposure of lancet (evaluate exposure only where lancet is medial to side plates, not at adoral tip where no side plates are present)
    0 = lancet not exposed between side plates
    1 = lancet exposed less than half width of ambulacrum
    2 = lancet exposed for half or more than half width of ambulacrum
32. Location of widest exposed portion of lancet (evaluate curved ambulacral length from aboral tip to center of mouth)
    0 = lancet widest at oral third of ambulacrum
    1 = lancet widest below oral third of ambulacrum
33. Serrations on lateral edges of lancet
    0 = absent
    1 = present
34. Plates surrounding ambulacrum (ambulacral length measured from aboral tip to center of mouth)
    0 = deltoids surround greater length of ambulacra than do radials
    1 = radials surround equal or greater length than deltoids
35. Plates bearing median groove (evaluate length from oral end of lancet to aboral end of ambulacrum)
    0 = lancet bears median groove over more than half length of ambulacrum
    1 = side plates bear median groove over more than half length of ambulacrum but not over entire region of ambulacrum along which side plates are developed
    2 = side plates bear median groove wherever present (lancet only bears groove adoral to adoral-most side plate)

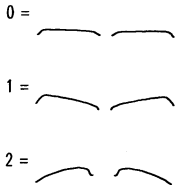

FIG. A4—Profiles of transverse sections of ambulacra, illustrating states of character 26. Exterior of specimen is toward top of page.

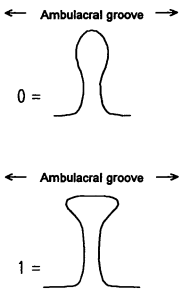

FIG. A5—Single cover plate lobes in plan view, illustrating states in character 41. Top of lobe borders on ambulacral groove.

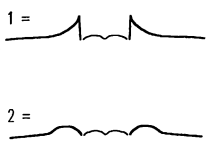

FIG. A6—Transverse cross sections of ambulacral and radial plates illustrating states of character 53. Thick lines indicate ambulacral margin. Thin lines represent ambulacrum. Exterior of specimen is toward top of page.

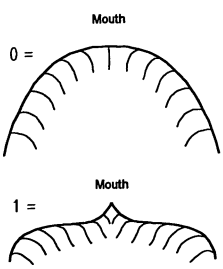

FIG. A7—Adoral tip of deltoid lip, illustrating states of character 57. Hatchures indicate curvature of surface of lip.

36. Curvature of medial ends of side grooves
    0 = curve adorally
    1 = do not curve adorally
37. Coincidence of side grooves and side plate sutures (whenever possible, coded for plates on adoral half of ambulacrum; ignore outer side plates when coding)
    0 = sutures between side plates coincide with side grooves
    1 = sutures between side plates alternate with side grooves
38. Cover plate lobes prominent on both lateral margins of side groove (only applicable for specimens with lobes present on side grooves)
    0 = lobes border side groove adorally
    1 = lobes border both sides of side groove
39. Cover plate lobes along side grooves (coding here is equivalent to adding absent state to character 38; a lobe is considered to border lateral food groove if axis of lobe intersects lateral groove rather than median food groove)
    0 = absent
    1 = present
40. Reduced D ambulacrum
    0 = not reduced in length
    1 = reduced in length
41. Shape of median groove cover plate lobes (see Figure A5; concentrating on adoral-most 2-3 lobes)
    0 = lobes elongate, rounded, or clavate
    1 = lobe ends expanded, angular, flattened
42. Cover plate lobes extend adorally beyond side plates
    0 = lobes do not occur beyond side plates
    1 = lobes occur beyond side plates
43. Number of pores per side plate along deltoids (not applicable for specimens lacking pores of any kind)
    0 = 0
    1 = 1
    2 = 2
44. Number of pores per side plate along radials (not applicable for specimens lacking pores of any kind)
    0 = 5-7
    1 = 1
    2 = 2
45. Length of combined side plates and outer side plates (evaluate length from extreme points on plate in plan view, paralleling boundaries between side plates)
    0 = length less than 1.5 times width
    1 = length greater than 1.5 times width but less than 2.5 times width
    2 = length greater than 2.5 times width
46. Angle of combined side plates and outer side plates (coded for largest side plates, near adoral end; direction of skew constant on all specimens observed)
    0 = perpendicular to midline of ambulacrum, within 10°
    1 = side plates skewed
47. Side plate elevation
    0 = side plate surfaces elevated above surface of lancet
    1 = side plates' upper surfaces flush with lancet
    2 = both conditions on 1 specimen
48. Side plates surround outer side plates (if pore forms part of boundary around outer side plate, consider surrounded)
    0 = do not surround outer side plates
    1 = surround outer side plates on mature portions of ambulacrum

49. Position of outer side plate relative to side plate (evaluate embayment of side plates by using medial portion of sutures between side plates to define general side plate shape, and then judge how outer side plates impinge on this shape)
    0 = outer side plate aboral to side plate
    1 = outer side plate adoral to side plate
    2 = outer side plate exactly between 2 side plates
50. Size of outer side plates (comparing external exposure)
    0 = outer side plates less than half size of side plates
    1 = outer side plates more than half size of side plates
51. Extent of outer side plates at lateral margin of ambulacrum
    0 = lateral edges of outer side plates do not touch
    1 = lateral edges of outer side plates touch
52. Medial extent of outer side plates
    0 = Outer side plates do not extend to lancet
    1 = Outer side plates extend to lancet
53. Radials and/or deltoids thicken at ambulacral margin (see Figure A6)
    0 = thickening absent
    1 = serif developed along ambulacral margin
    2 = broad ridge developed at ambulacral margin
54. Regular deltoids contribute to outer thecal wall
    0 = deltoids form a portion of outer thecal wall, with some portion of the sutures between a deltoid and the two adjacent radials lying on the same smooth surface, not separated by a sharp ridge
    1 = interradially disposed portions of DR sutures are separated by a sharp ridge, nowhere lying in the same plane on a single, smooth outer thecal surface
55. Exposure of anal deltoid (just one anal deltoid, not all, need be exposed; use criteria from character 54 to determine whether contributes to outer thecal surface)
    0 = anal deltoid does not contribute to external wall
    1 = anal deltoid contributes to external wall
56. Adoral opening to hydrospire folds formed solely by deltoid
    0 = deltoid does not completely form opening
    1 = opening formed solely by deltoid
57. Deltoid lip forms adoral spout (see Figure A7; inner, aboral edge of lip must be recurved, forming a point directed toward mouth, not just having a point at exterior)
    0 = absent
    1 = present
58. Deltoid prong (see Figure A8; define prong as adoral end of deltoid which is reflected abaxially and elevated above oral surface)
    0 = absent
    1 = present
59. Concavity in aboral side of deltoid lip (coding an indentation or depression between elevated wings of deltoid lip)
    0 = absent
    1 = present
60. Deltoid crest (define crest as a sharp ridge between those portions, within the ambulacral sinus, of two DR sectors of a deltoid which are not lying in the same plane [modified from Breimer and Macurda, 1972])
    0 = absent
    1 = present
61. DD [deltoid-deltoid] growth sector (evaluate surface area in each sector)
    0 = DD sector small; not tabular; very narrowly V-shaped
    1 = DD sector well developed, but smaller than DR sector; typically chevron-shaped
    2 = DD sector sub-equal to or larger than DR sector
62. High ridge between DR and DD sectors
    0 = absent
    1 = present

63. Location of anal opening
    0 = at suture between radials and anal deltoids
    1 = within anal deltoids
64. Inflated anal deltoid (inflated includes projecting above oral surface higher than other deltoids)
    0 = anal deltoid same thickness as regular deltoids
    1 = anal deltoid swollen
65. Anal deltoids (ordered)
    0 = single plate
    1 = two plates
    2 = U-shaped plate(s) with aborally-directed limbs, located between adoral and aboral plates
    3 = five plates
66. Condition of intercalated anal deltoid plate(s)
    0 = subdeltoid (single plate intercalated between adoral and aboral plates)
    1 = cryptodeltoids
67. Cryptodeltoid exposure (concealment is within other anal deltoids, not just beneath side plates)
    0 = cryptodeltoids concealed within other anal deltoids
    1 = cryptodeltoids exposed externally
    2 = C cryptodeltoid exposed, D hidden
68. Cryptodeltoids touch at exterior
    0 = cryptodeltoids do not meet at exterior
    1 = cryptodeltoids meet at exterior
69. Pit at deltoid-radial-radial triple junction
    0 = absent
    1 = present
70. Radial-deltoid overlap (evaluate suture relative to external surfaces of radials and deltoids; the plate making the more acute angle with the suture is considered to be the overlapping plate)
    0 = plates abut
    1 = radial overlap
    2 = deltoid overlap
71. Radial limbs projecting above level of oral surface
    0 = absent
    1 = present
72. Prominent radial lip (define lip as thickening of radial at aboral end of sinus, often with evidence of incremental growth, continuing the profile of the pelvis; lip should be larger than any general thickening at ambulacral margin coded in character 53)
    0 = absent
    1 = present
73. Radial prong (define prong as elongation of radial by addition of secondary calcite at end of ambulacrum; prong is larger-scale feature than radial lip)
    0 = absent
    1 = present
74. Radial - RA growth front (define RA [radial-ambulacral] growth front as front from origin of radial toward tip of ambulacrum; this represents space filling by radial between radial and ambulacral tip to compensate for growth along RD growth front)
    0 = absent
    1 = present
75. Angle of intersection of radial surfaces (see Figure A9; evaluate large-scale, structural relationship of radials to one another, not local details of suture)
    0 = thecal surface smooth across intersection of radials
    1 = surfaces of radials form sharp, concave angle
    2 = surfaces of radials form sharp, convex angle
76. Radial-radial suture (see Figure A10; smaller-scale feature than character 75)
    0 = suture undifferentiated from rest of radial's surface
    1 = suture indented
    2 = suture swollen

FIG. A8—Tangential view of side of deltoid plate in ambulacral sinus, looking across top of specimen. Arrow indicates deltoid prong of character 58.

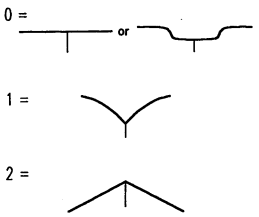

FIG. A9—Transverse cross sections of sutures between radial plates, illustrating states of character 75. Heavy lines are outer surfaces of radials; light lines are sutures between radials. Drawings depict approximately 1/20th thecal circumference.

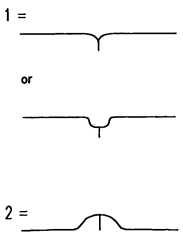

FIG. A10—Transverse cross sections of radial-radial sutures illustrating states of character 76. Width of drawing is approximately 1/40th thecal circumference. Exterior of specimen is toward top of page.

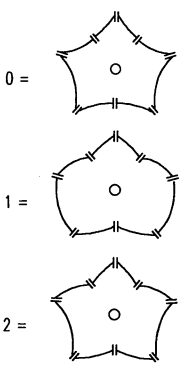

FIG. A11—Basal view of radial-basal sutures, illustrating states in character 77. Gaps in outlines indicate boundaries between 8 growth sectors along sutures. Circle is stem facet. AB interray is oriented toward top of page.

77. Curvature of individual basal-radial sutures in basal view (see Figure A11; coding curvature of individual sutures between growth sectors rather than considering overall outline)
    0 = sutures concave
    1 = sutures convex
    2 = Basal-C radial and basal-E radial sutures concave, others convex
78. Basal plate reduction
    0 = 2 basal plates
    1 = 3 basal plates
79. Position of azygous basal
    0 = AB interray
    1 = DE interray
80. Modification of basals at stem attachment area (state 80.0 reflects growth perpendicular to rather than parallel with stem axis; define BA [basal/attachment area] growth front as front extending from origin of basal toward attachment area; origin of basal will typically be adoral to attachment surface for state 80.1; only applies to species with stems)
    0 = no aborally-directed modification
    1 = BA growth front
    2 = secondary deposits on basals
81. Proximal stem elements
    0 = stem composed of button-like columnals
    1 = proximal stem elements solid, fused, or very elongate
    2 = no stem
82. Stem attachment scar (not applicable for specimens lacking stems)
    0 = circular scar
    1 = triangular scar
    2 = "cloven" basal at point of attachment
83. Growth lines on plates (define growth lines as regularly spaced and laterally continuous features paralleling plate boundaries, not randomly spaced ornamentation; may be subject to poor preservation)
    0 = absent
    1 = present
84. Growth line character (not applicable for specimens without growth lines)
    0 = straight: very fine and regular
    1 = wavy
    2 = nodular (rows of nodes)
    3 = straight: coarse, rugose, not regularly spaced
85. Ornamentation (features present as integral parts of growth lines are not considered ornamentation)
    0 = absent
    1 = straight
    2 = nodular
    3 = star-shaped
    4 = straight ridges produced by effect of ambulacrum on growth field
    5 = reticulate, pitted sculpture
86. Sharp ridges connecting tips of ambulacra to basal triangle (ridges occur at center of each growth sector in pelvis)
    0 = present
    1 = absent
87. Basal chord (ordered; compare with 101 and 100; calculated from Foote's, 1991, data; distance from point 1 to average of points 3 and 4, with distance from point 1 to point 7 standardized to unit length)
    0 = less than 0.20 length of oral-aboral axis
    1 = greater than 0.20 but less than 0.33 length of oral-aboral axis
    2 = greater than 0.33 but less than 0.50 length of oral-aboral axis
    3 = greater than 0.50 length of oral-aboral axis

88. Radial chord (ordered; compare with 99 and 100; calculated from Foote's, 1991, data; distance from point 2 to average of points 5 and 6, with distance from point 1 to point 7 standardized to unit length)
    0 = less than 0.20 length of oral-aboral axis
    1 = greater than 0.20 but less than 0.45 length of oral-aboral axis
    2 = greater than 0.45 but less than 0.80 length of oral-aboral axis
    3 = greater than 0.80 length of oral-aboral axis
89. Deltoid chord (ordered; compare with 99; calculated from Foote's, 1991, data; distance from average of points 5 and 6 to point 7, with distance from point 1 to point 7 standardized to unit length)
    0 = less than 0.45 length of oral-aboral axis
    1 = greater than 0.45 but less than 0.75 length of oral-aboral axis
    2 = greater than 0.75 length of oral-aboral axis
90. Chord of radial in pelvis (ordered; compare with 101; calculated from Foote's, 1991, data; distance from point 7 to point 8, with distance from point 1 to point 7 standardized to unit length)
    0 = less than 0.33 length of oral-aboral axis
    1 = greater than 0.33 but less than 0.60 length of oral-aboral axis
    2 = greater than 0.60 length of oral-aboral axis
91. Ambulacral chord (ordered; compare with 98; calculated from Foote's, 1991, data; distance from point 1 to average of points 3 and 4, with distance from point 1 to point 7 standardized to unit length)
    0 = less than 0.60 length of oral-aboral axis
    1 = greater than 0.60 but less than 1.00 length of oral-aboral axis
    2 = greater than 1.00 length of oral-aboral axis
92. Plunge of basal *c* axes (plunges are of *c* axes projected to the lower hemisphere; state coded represents the majority state for the three basals in each specimen; coding makes states larger than largest observed intraspecific variation in *c* axis orientation)
    0 = majority of axes less than 30° in axial or abaxial direction
    1 = majority of axes between 30° and 90° in abaxial direction
    2 = majority of axes between 90° and 30° in axial direction
93. Plunge of radial *c* axes (plunges are of *c* axes projected to the lower hemisphere; state coded represents the majority state for the five radials in each specimen; coding makes states larger than largest observed intraspecific variation in *c* axis orientation)
    0 = 50° to 0° in axial or 0° to 10° in abaxial direction
    1 = 10° to 70° in abaxial direction
    2 = 70° to 90° in abaxial or 90° to 50° in axial direction
94. Plunge of regular deltoid *c* axes (plunges are of *c* axes projected to the lower hemisphere; state coded represents the majority state for the four regular deltoids in each specimen; coding makes states larger than largest observed intraspecific variation in *c* axis orientation except for 94.3, coded because of structured variation among axes from different interrays)
    0 = majority of axes less than 30° in axial or abaxial direction
    1 = majority of axes between 30° and 90° in abaxial direction
    2 = majority of axes between 90° and 30° in axial direction
    3 = axes from A and E deltoids plunge abaxially, B and D deltoids plunge axially
95. Stratigraphic range
    See Figure 7 and discussion in text
96. Posterior C-ray hydrospire folds
    0 = folds absent in posterior C hydrospire field
    1 = folds present but reduced in number
    2 = folds present in full number
97. Posterior D-ray hydrospire folds
    0 = folds absent in posterior C hydrospire field
    1 = folds present but reduced in number
    2 = folds present in full number

98. Length of ambulacra (ambulacral length and half circumference of theca measured as curved lengths)
    0 = length less than half semicircumference of theca
    1 = length more than half semicircumference of theca
99. Relative length of radials versus deltoids (measure lengths parallel to polar axis, from extreme points visible in lateral view on each plate)
    0 = radials longer than deltoids
    1 = deltoids longer than radials
100. Relative length of basals versus radials (measure lengths parallel to polar axis, from extreme points visible in lateral view on each plate; indented basals are considered short)
    0 = radials longer than basals
    1 = basals longer than radials
101. Relative length of basals versus radials in pelvis (measured from base of theca to aboral ambulacral tips, parallel to polar axis, with radial-basal juncture located at the level of the midpoint between adoral-most extent of basals and aboral-most extent of radials)
    0 = radials longer than basals
    1 = basals longer than radials
102. Epideltoid
    0 = epideltoid absent
    1 = epideltoid present
103. Hypodeltoid
    0 = hypodeltoid absent
    1 = hypodeltoid present
104. Cryptodeltoids
    0 = cryptodeltoids absent
    1 = cryptodeltoids present
105. Paradeltoid
    0 = absent
    1 = present
106. Subdeltoid
    0 = subdeltoid absent
    1 = subdeltoid present